Icarus 445 (2026) 116828

Contents lists available at ScienceDirect

Icarus

journal homepage: www.elsevier.com/locate/icarus

Liquid Vein networks as habitats in ice-cemented ground on Earth and Mars: Effects of soil geometry and salts☆

H.G. Sizemore [a,*], M.T. Mellon [b], A.W. Rempel [c], C.P. McKay [d], J.L. Heldmann [d], C.R. Stoker [d], M.R. Perry [a]

[a] Planetary Science Institute, Tucson, AZ 85719, United States of America
[b] Cornell University, Ithaca, NY 14583, United States of America
[c] University of Oregon, Eugene, OR 97403, United States of America
[d] NASA Ames Research Center, Moffett Field, CA 94035, United States of America

ARTICLE INFO

Keywords:
Permafrost
Habitability
Mars
Earth

ABSTRACT

We have carried out simulations of permafrost liquid fraction to investigate the historical habitability of Martian and Antarctic ground ice. These simulations are based on the development of new soil freezing curves (SFCs) for example Martian and Antarctic soils, and expand upon our previous investigation of the temperature history of shallow Martian ice (Mellon et al., 2024). We considered the effects of salt doping on both soil types, using magnesium perchlorate, $Mg(ClO_4)_2$, as an endmember low-eutectic-temperature solute representative of Mars, and NaCl as a high-eutectic-temperature endmember, approximately representative of solutes in the Dry Valleys of Antarctica. We applied our SFCs to calculate the total liquid fraction, S_l, and maximum liquid vein diameter (or refugia diameter), d_r, in the icy permafrost under relevant Martian and Antarctic environmental conditions, building on previous work that considered habitability limits in the context of temperature, T, and water activity, a_w, only. We defined habitability thresholds of $S_l \geq 5$ % and $d_r \geq 1$ μm, then examined which of four habitability metrics (T, a_w, S_l, d_r) presents the dominant limitation to shallow ice habitability in the Martian icy-permafrost environment and in the perennially sub-freezing environments of the Antarctic Dry Valleys. We also re-evaluated optimal landing site selection for Mars life and habitability exploration missions in this context.

We find that, without salts, neither of the examined soils produce habitable values of S_l or d_r below ~ -3 °C based on pore-confinement effects alone. The addition of 1 dry wt% NaCl extends the occurrence of habitable values of S_l and d_r to the eutectic temperature of −21 °C; the addition of 1 dry wt% $Mg(ClO_4)_2$ extends the occurrence of habitable values of S_l and d_r to the magnesium perchlorate eutectic temperature of −64 °C, well below the previously defined extreme metabolic limit of $T = -40$ °C. In both the Antarctic Dry Valley and Martian environments solute concentration is spatially variable and can occur locally at more or less than the 1 wt% scenarios we investigated. In the case of localized solute deficits, habitable S_l and d_r may not be achieved, even during summertime and high-obliquity temperature excursions. However, meeting the requirement of $d_r >$ 1 μm and $S_l > 5$ % is surprisingly easy for silty to sandy soils with plausible salt doping in both the Martian and Antarctic summertime environments. Further, our simulations indicate that for soils found at the Phoenix landing site, 1 wt% $Mg(ClO_4)_2$ produces $S_l \sim 6$ % and $d_r > 5$ μm poleward of ~50°N in the current Martian climate.

Our new results re-enforce our previous landing site recommendations for Mars habitability missions (Mellon et al., 2024), indicating that progressively higher northern latitudes offer progressively better opportunities to sample "warmer" ice, which has met or exceeded multiple habitability metrics for extended time periods.

1. Introduction

Much of the long-term interest in the habitability of Mars has centered on the distant geologic past when surface conditions may have been more clement and possibly supported life. Discussions of modern habitability and extant life have largely focused on deep subsurface

☆ This article is part of a Special issue entitled: 'Mars Polar Science' published in Icarus.

* Corresponding author at: Planetary Science Institute, 1700 East Fort Lowell, Suite 106, Tucson, AZ 85719-2395, United States of America.
E-mail address: sizemore@psi.edu (H.G. Sizemore).

https://doi.org/10.1016/j.icarus.2025.116828
Received 21 January 2025; Received in revised form 7 September 2025; Accepted 22 September 2025
Available online 10 October 2025
0019-1035/© 2025 The Authors. Published by Elsevier Inc. This is an open access article under the CC BY-NC-ND license (http://creativecommons.org/licenses/by-nc-nd/4.0/).

environments to provide the requisite heat, water, and radiation protection for organisms. However, renewed interest in shallowly buried ground ice as a target for future robotic missions (Putzig et al., 2019; National Academies of Sciences, Engineering, and Medicine, 2023) and a resource for future human missions (Piqueux et al., 2019; Morgan et al., 2021; Heldmann et al., 2022; Putzig et al., 2023) demands a detailed reconsideration of ice-rich permafrost as a possible Martian habitat.

We recently assessed the historical habitability of shallowly buried Martian ice using simulations of ice temperature (Mellon et al., 2024). Our earlier work focused on ice accessible to bore hole science via landed drills and made specific recommendations for landing site selection for life detection experiments. Our modeling approach (Mellon et al., 2024) improved upon earlier studies by Jakosky et al. (2003) and Zent (2008), by updating the parameterization of historical near-surface water vapor density based on in situ data and by computing the water activity, a_w, of the ice as a habitability metric, in addition to temperature, T.

Multiple studies of Martian habitability and special regions (summarized by Rummel et al., 2014) have highlighted $a_w \sim 0.6$ as a consistent lower limit for terrestrial microorganisms to thrive and propagate, although survival and maintenance metabolism may be possible at lower a_w. Anabolic activity has been detected at water activity as low as $a_w = 0.54$ in seawater-sourced brines (Paris et al., 2023), but this extension of the habitable limit is likely not appropriate to polyextreme environments such as Mars (Fox-Powell et al., 2016; Paris et al., 2023). A minimum temperature threshold of −18 °C has been commonly cited for for growth and propagation (e.g., Rummel et al., 2014), although Rivkina et al. (2000) observed a stationary growth phase for bacteria in Siberian permafrost at —20 °C, and some organisms can readily metabolize and maintain cell function and repair down to about −33 °C (e.g., Bakermans and Skidmore, 2011). Several studies have demonstrated evidence of metabolism through respiration, nitrification, carbon turnover, and photosynthesis as low as −40 °C (Sowers, 2001; Panikov et al., 2006; de Vera et al., 2014). Furthermore, Price and Sowers (2004) argued that −40 °C may not represent a cutoff limit, but that rates of metabolism slow exponentially with temperature, along with the rates of molecular decay that require repair. However, Clarke et al. (2013) expressed concern that vitrification of cytoplasm may inhibit metabolism at temperatures above −40 °C, though this limit depends on the presence of antifreeze proteins (Bakermans, 2008). As such, we previously considered habitability down to an "extreme metabolic limit" of $a_w > 0.6$ and $T > -40$ °C, while noting that the temperature represents the more restrictive constraint (Mellon et al., 2024). We adopt the same standards in our current work.

Jakosky et al. (2003) and Zent (2008) explicitly assumed that near-surface habitability was contingent on the presence of a network of liquid veins in the ice-soil matrix at temperatures well below bulk freezing (0 °C). Both studies also shared the assumption that the volume and connectedness of liquid vein networks were potentially limiting for microbial survival. They used temperature as a proxy for liquid availability, based on laboratory experiments indicating that the growth of Arctic bacterial populations at subfreezing temperatures was halted, or reached a stationary phase, when the reduction of residual liquid in the host permafrost by progressive freezing limited the efficient diffusion of nutrients to the cells (Rivkina et al., 2000).

To establish their low temperature thresholds for habitability, Jakosky et al. (2003) and Zent (2008) relied on a limited set of empirical soil freezing curves (SFCs) available for terrestrial soils at that time. In their discussion of habitability thresholds, Jakosky et al. (2003) and Zent (2008) also noted a variety of reports of minimum temperatures at which metabolism had been observed for psychrophilic bacteria, but these studies did not include independent information on subfreezing liquid availability and nutrient transport (see Rivkina et al., 2000; Beaty et al., 2005; and Rummel et al., 2014, for similar discussions).

Recent substantial progress in the understanding of soil freezing now allows for predictive modeling of the liquid content of frozen Martian and terrestrial soils (Sizemore et al., 2015; Chen et al., 2020; Lei et al., 2022). Here, we expand on our earlier work characterizing the temperature and water activity of shallow Martian ice (Mellon et al., 2024) to directly calculate the total liquid fraction, S_l, and maximum liquid vein diameter (or "refugia diameter," d_r) in representative "Martian" and "Antarctic" ice-cemented soils under relevant environmental conditions. We define habitability thresholds for these two parameters, based on the work of Rivkina et al. (2000) and others, assuming specifically, that: (1) a liquid vein network is connected enough to allow transport of nutrients and wastes for $S_l > 5$ %; and (2) refugia diameter should exceed the size of approximately micron-scale cellular organisms to allow full immersion of single cell organisms in "liquid." In this context, we examine which of four habitability metrics (T, a_w, S_l, d_r) presents the dominant limitation to shallow ice habitability in the Martian icy-permafrost environment and in the perennially sub-freezing environments of the Antarctic Dry Valleys. We also revisit discussion of optimal landing site selection for Mars life and habitability exploration missions in this context.

2. Background: Liquid films in ice-cemented soil

During the decade and a half separating the surveys of historical ice habitability by Zent (2008) and Mellon et al. (2024), two major developments expanded our understanding of liquid water availability in shallow Martian permafrost. First, perchlorate salts were discovered at the Phoenix (Hecht et al., 2009; Stillman and Grimm, 2011), Curiosity (e.g., Archer et al., 2013; Ming and 449 co-authors, 2013; Sutter et al., 2017), and Perseverance (Farley and 117 co-authors, 2022; Scheller and 65 co-authors, 2022) landing sites on Mars. The wide geographic distribution of these detections, combined with evidence of trace amounts of perchlorate in Martian meteorites (Kounaves et al., 2014; Jaramillo et al., 2019), and the existence of multiple pathways for Martian perchlorate production (Catling et al., 2010; Steele et al., 2018; Carrier and Kounaves, 2015; Qu et al., 2022) collectively suggest that deliquescent salts are ubiquitous in Martian soils, and may contribute to wide-spread freezing point depression and localized formation of metastable liquid brines. Numerous subsequent studies have sought to characterize the exotic properties and behavior of pure perchlorate brines under Mars-relevant conditions (e.g., Chevrier et al., 2009; Hecht et al., 2009; Fischer et al., 2014, Fischer and Martínez, 2016; Gough et al., 2011, Gough et al., 2023; Toner et al., 2014a, 2014b; Toner et al., 2015; Nuding et al., 2014, 2015; Nikolakakos & Whiteway 2015; Toner and Catling, 2018; Rivera-Valentín et al., 2018; Rivera-Valentín et al., 2020). The discovery and intense investigation of perchlorates has occurred in the context of extensive evidence indicating other soluble salts are ubiquitous and abundant in Martian soils. Sulfates and chlorides have been detected at every Martian landing site, beginning with Viking, as have weakly and strongly cemented soil crusts consistent with salt cementation. Nitrates have also been detected extensively at the Curiosity and Perseverance landing sites (e.g., Stern et al., 2017; Archer et al., 2024). These less-exotic salts cause significant freezing point depression in their own right (e.g., Gough et al., 2016). Thus, a fully comprehensive consideration of residual water in Martian permafrost would need to account for the cumulative effects of solutes with a range of eutectic temperatures (see Table 1) and their complex interactions.

Second, and in parallel with investigations of perchlorates, theoretical and laboratory studies have expanded the library of Mars-relevant soil freezing curves (SFCs) and improved confidence in predicted low temperature soil freezing behavior (e.g., Sizemore et al., 2015; Chen et al., 2020; Lei et al., 2022). SFCs describe the residual liquid fraction, S_l, in the pores of H_2O-saturated soil (liquid + ice + soil) at temperatures below 0 °C. This unfrozen water persists at low temperature even in the absence of soluble impurities due to a combination of interfacial melting (the molecular disorder that occurs at the flat interface between crystalline ice and a foreign substrate, e.g. a soil particle), grain boundary

Table 1
Environmentally available salts and acids that may contribute to freezing point suppression and residual soil pore water on Mars and in the Antarctic Dry Valleys.

Species	Eutectic [C]	Eutectic [K]	Reference
$NaSO_4$	−1.2	271.95	Bass 1980
$MgSO_4$	−3.5	269.65	Bass 1980
$Mg(NO_3)_2$	−16.8	256.35	Morillon et al. 1999
NaCl	−21.2	251.95	Hall et al. 1988
$MgCl_2$	−33.6	239.55	Morillon et al. 1999
$CaCl_2$	−49.8	223.35	Marcus 2017
$Mg(ClO_4)_2$	−68.6	204.55	Marcus 2017
$Ca(ClO_4)_2$	−74.4	198.75	Toner et al. 2014a
LiCl	−74.8	198.35	Morillon et al. 1999
H_2SO_4*	−84	189.15	Rempel et al. 2001a; Weast, 1987
H_2SO_4*	−73	200.15	Price, 2000
HCl	−88	185.15	Price, 2000
HNO_3	−43	230.15	Price, 2000
CH_3SO_3H	−75	198.15	Price, 2000
CH_2O_2	−49	224.15	Price, 2000

melting (melting at the interface between two crystals of the same substance), and the Gibbs-Thomson effect (melting along a curved interface between a solid and its melt). Details of the molecular interactions that give rise to this unfrozen or "premelted" water are described by Dash et al. (2006) and Wettlaufer and Worster (2006). Fig. 1 shows a schematic of ice and residual liquid in an idealized soil pore. Thin films separate crystalline pore ice from adjacent soil particles due to interfacial premelting, but under habitable conditions S_l is dominated by larger veins of residual liquid produced by the Gibbs-Thomson effect near soil grain contacts. A similar network of liquid veins can occur in crystalline ice itself due to grain boundary melting and environmentally available acids (e.g., Fukazawa et al., 1998; Price, 2000; Rempel et al., 2001a, 2001b).

In freezing soils, Rempel et al. (2001a, 2001b) recognized that gradients in the strengths of ice-soil interactions produce a net thermomolecular buoyancy force on the ice-soil matrix. This insight led to the development of predictive models of terrestrial ice lens growth and frost heave (Rempel et al., 2004; Rempel, 2007, 2008, 2012). In developing his terrestrial frost heave model, Rempel (2007) relied on power-law parametrizations of empirical SFCs compiled by Andersland and Ladanyi (2004) from a disparate set of early laboratory and field studies. Note that the individual SFCs invoked by Jakosky et al. (2003) and Zent (2008) to argue that liquid water could persist in Martian soils in the range $T \sim -20$ °C to 0 °C are included in the Anderland and Ladanyi 2004 database. Sizemore et al. (2015) later applied a subset of these empirical SFCs to a model of Martian frost heave, and took the additional step of algebraically combining the power-law SFCs with liquidus curves for magnesium perchlorate, $Mg(ClO_4)_2$, and calcium perchlorate, $Ca(ClO_4)_2$, to approximate the freezing behavior of salty Martian soils. In the absence of solutes, interfacial premelting and the Gibbs-Thomson effect are the dominant sources of unfrozen water in porous media at temperatures below bulk melting. Based on their hybrid SFCs, Sizemore et al. (2015) argued that pore-space confinement (interfacial premelting and the Gibbs-Thomson effect) would remain dominant in salt-doped clays, but that colligative effects (i.e. freezing point depression due to salts) would dominate liquid availability in silts and sands. However, their smooth SFCs did not capture possible sharp changes in S_l at or below the eutectic temperature.

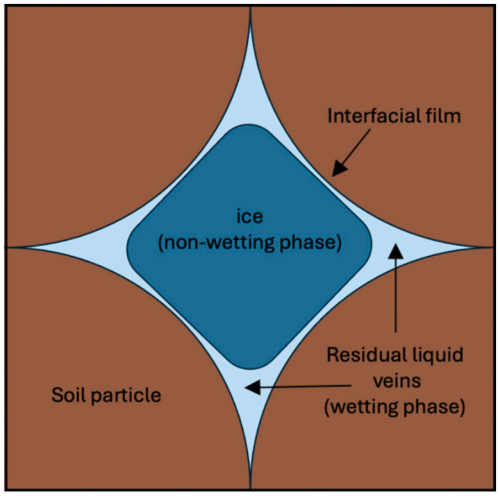


Fig. 1. Schematic of residual liquid in the pore space of a frozen soil, modified from Chen et al. (2020). Premelted interfacial films separate pore ice from mineral surfaces everywhere, but residual liquid volume is dominated by larger veins of liquid produced by the Gibbs-Thomson effect near mineral-grain contacts.

A variety of geophysical applications have driven subsequent efforts to (1) validate the choice of a power-law relationship to represent historical and recent soil freezing data and (2) directly measure the total liquid fraction $S_l(T)$ in natural soils and controlled bead-packs with salt doping (e.g., Dash et al., 2006; Rempel, 2008). Chen et al. (2020) developed a numerical approach to building SFCs for a variety of soil-particle geometries, with and without salt doping. They used a Monte Carlo approach to sample the pore space in a synthetic 3D packing of poly-dispersed spherical particles and evaluated local geometric constraints that allowed them to assess changes in the relative proportions of pore fluid and ice with changing temperature. They validated their model extensively against laboratory data for: i) ice-water equilibrium in graphitized carbon black and polystyrene powders; ii) liquid retention in the vadose zone for natural silts and loams; and iii) mercury porosimetry analysis of natural sands from Beacon Valley, Antarctica. Broadly, Chen et al. (2020) demonstrated that their Monte Carlo approach predicted pore space phase partitioning in irregular porous media accurately, despite the idealized assumption of spherical particles. They also demonstrated that a power-law approximation was reasonable for a variety of SFCs relevant to Martian and Antarctic soils above the eutectic temperature of a given solute. Separately, Lei et al. (2022) used nuclear magnetic resonance (NMR) relaxation, self-diffusion measurements, and magnetic resonance imaging (MRI) to characterize the structure and volume of liquid vein networks in frozen brines and saturated mono-disperse bead packs. They specifically investigated magnesium chloride, $MgCl_2$, concentrations of 15, 30, and 60 mM and spherical poly-methyl methacrylate (PMMA) particles of diameter 0.4, 9.9, and 102.2 μm. They compared their laboratory data to the Chen et al. (2020) Monte Carlo model, allowing for further validation and refinement of physical assumptions in the model. They also documented time-variable effects such as grain ripening and hysteresis in $S_l(T)$ that are outside the capabilities of current predictive freezing models. (See Discussion.)

Laboratory studies characterizing the freezing behavior of brines and brine-soil mixtures have long suggested that a wide array of geologically relevant salts could inhibit freezing in the Martian environment (e.g., Table 1), but the presence of $Mg(ClO_4)_2$ and/or $Ca(ClO_4)_2$ might offer unique advantages to Martian organisms. Toner et al. (2014a) observed that, in contrast to four other salt solutions they investigated, magnesium and calcium perchlorate solutions never crystallized during slow cooling, but remained in a supercooled, liquid state until forming an amorphous glass near −120 °C (153 K) – i.e. neither ice crystals nor excluded salt crystals developed at any temperature. The occurrence of this amorphous glass phase might improve the survivability of extreme low-temperature periods on Mars by mitigating the risk of cell damage from ice crystal formation. This astrobiological advantage occurs in addition to the well-documented low eutectic temperatures of perchlorate brines, and their tendency to produce significant supercooling below the eutectic temperature of ∼ − 64 °C (209 K) for $Mg(ClO_4)_2$. Note that supercooling has introduced ambiguity in laboratory

experiments to determine perchlorate eutectics (Stillman et al., 2019; Chevrier et al., 2009; Toner et al., 2014a; Toner et al., 2015). More recent experiments suggest that supercooling and the inhibition of crystal formation may be enhanced in perchlorate-brine / regolith mixtures, while still allowing for the maintenance of habitable values of water activity (Shumway et al., 2023). Some caution is warranted in considering the effects of perchlorates on low-temperature habitability, as high perchlorate concentrations can be toxic even to organisms that metabolize perchlorate (Heinz et al., 2021). However, intimate mixing of perchlorate salts in ice-cemented permafrost may create a unique niche in the perennially frozen Martian environment. Further, the preceding arguments are based on the properties of single-salt solutions, although binary or multi-salt mixtures may further improve the liquid stability of a system (e.g., Gough et al., 2014) without invoking a supercooled liquid.

There has been long-term interest in liquid vein networks as habitats in ice-rich permafrost, because of their ability to facilitate mass transfer. Ostroumov and Siegert (1996) demonstrated that networks of residual liquid in frozen loams and rocks allowed for substantial diffusion of dissolved ions, relative to much more restricted ion transport in pure-ice lenses and low-permeability rock. They argued that the occurrence of highly permeable microzones in permafrost supported the hypothesis that sub-freezing mass transfer could allow exchange of liquid water and ions between living cells and the habitat, permitting metabolism, and opening the possibility of long-term survival of viable microorganisms in permafrost on Mars, asteroids, and comets. Price (2000) modeled the development of liquid vein networks in subglacial ice at Lake Vostok, Antarctica. He approximated the population of motile micron-scale bacteria that could be supported by liquid veins in deep, clear lake ice, and proposed experiments to detect this population of bacteria. Rempel et al., 2001a modeled the migration of climate markers through liquid veins in ice cores from Greenland and Antarctica and concluded that the diffusion of impurities through the liquid vein network, though slow, could result in the displacement of climate markers by 10s of cm relative to equivalent age ice on hundred-thousand-year timescales. Rivkina et al. (2000) measured metabolic activity in laboratory samples of Siberian permafrost and observed a correlation between the temperatures at which bacterial growth reached a stationary phase in their experiments and the temperature dependence of liquid fraction in permafrost measured by Ostroumov and Siegert (1996). Based on this correlation, Rivkina et al. (2000) concluded that thinning of liquid veins with reduced temperature progressively restricted diffusion of nutrients, limiting bacterial growth.

It is important to note that liquid vein networks occur at subfreezing temperatures in both “clean” ice and ice-cemented soil, but we have chosen to focus on soils. There are several reasons for this choice. First, prediction of the liquid fraction and its geometric distribution in the confined pore space of a soil is better constrained than prediction of the volume and geometry of liquid films at ice-crystal boundaries in clean ice. In the latter case, the volume and character of the liquid vein network is strongly dependent on the specific soluble impurities entrained in the ice, as well as the temperature and pressure history of the ice, which will influence ice-grain size and vein diameter via grain-ripening (e.g., Price, 2000; Lei et al., 2022). Second, absent confinement effects of the soil pore space, clean low-temperature ice will have a lower liquid fraction, lower permeability, and lower effective diffusion coefficients for ion transport than adjacent soil-ice mixtures (Ostroumov and Siegert, 1996). Third, although “clean” massive ice and ice-cemented soil are both widespread in the Martian high latitudes, the shallowest, warmest, and most accessible ice on present-day Mars is likely to be pore-filling ice that was deposited from the vapor phase (e.g., Mellon et al., 2004; Mellon et al., 2009; Schorghofer and Forget, 2012; Mellon and Sizemore, 2022). Intimate mixing of mineral grains, associated salts, ice, and residual liquid may also increase nutrient availability by simple proximity.

In considering the habitability of icy Martian permafrost, both Jakosky et al. (2003) and Zent (2008) assumed that liquid veins were the primary habitat and conduit for nutrient/waste transport in the ice-soil matrix. Continuing that logic in our current work – and capitalizing on the new capability of modeling both S_l and d_r of icy permafrost – we have defined relevant threshold values at which these parameters indicate habitable conditions and chosen representative soils and salts to reflect the range of likely Martian and Antarctic behaviors.

To define our habitability thresholds, we relied on the premelting and soil freezing literature, which is primarily oriented toward explaining macroscopic geophysical phenomena (e.g., frost heave, glacial freeze-on; Rempel et al., 2001a; Rempel, 2007, 2008) and has only been linked to questions of permafrost habitability in limited experiments (Ostroumov and Siegert, 1996; Rivkina et al., 2000; Jakosky et al., 2003). Collectively, this literature suggests that bulk transport of H_2O through the vein network becomes efficient as S_l approaches ~10 % (Dash et al., 2006; Rempel et al., 2001a, 2001b; Rempel, 2007, 2008; Israelachvili, 2011). Bulk transport of residual liquid can proceed at lower S_l and via nanometer to sub-micron veins, but transport rates will be slower (e.g., Sizemore et al., 2015). Diffusion of solutes through an approximately static vein network can also occur across macroscopic distances (decimeters) on long (~10^5 year) timescales due to temperature and concentration gradients (Rempel et al., 2001a). Both bulk movement of residual liquid and diffusive transport of specific solutes may be important for supplying nutrients and removing waste from psychrophilic bacteria in permafrost.

Rivkina et al. (2000) argued that nutrient diffusion through nanometer-scale interfacial films (as opposed to larger liquid veins; see Fig. 1) at the interface of the cell wall and surrounding ice was a determining factor for the rate of metabolism and the equilibrium bacterial population that could be supported in permafrost. They measured uptake of radioactive sodium acetate to quantify metabolic activity in native bacterial populations of Siberian permafrost incubated at temperatures ranging from 5 °C to −20 °C. In all cases, the natural bacterial population reached a stationary growth phase, defined as the equilibrium population at which the rate of cell growth equals the rate of cell death. The stationary growth phase indicates active metabolism and organisms that are *not* in a state of anabiosis. Rivkina et al. (2000) correlated the rate of sodium acetate uptake at each incubation temperature with the SFC of the bacteria’s native permafrost, a non-saline loamy soil in which particles <10 mm comprised 32 % of the dry soil by weight. They concluded that they had observed uptake consistent with metabolism at temperatures down to −20 °C, S_l ~ 2 %, and interfacial film thicknesses <0.5 nm. They further argued that metabolism was likely to persist at lower temperatures, lower residual liquid fractions, and thinner film thicknesses, but that measuring metabolism under those conditions was limited by the timescale of the experiments (> 550 days).

We adopted a threshold for habitability at $S_l > 5$ %, consistent with a major inflection in the slope of the Rivkina et al. (2000) Siberian permafrost SFC and a corresponding inflection in the curve describing the rate of sodium acetate uptake as a function of temperature in their bacterial population. A threshold of $S_l > 5$ % is also consistent with a transition from slow (10^3 to >10^5 years) to more efficient (10s of sols to 10s of years) bulk transport of unfrozen water in the shallow Martian permafrost (Sizemore et al., 2015). We consider the $S_l > 5$ % threshold conservative for two reasons. First, Rivkina et al. (2000) observed stationary growth at lower S_l, and secondly, a threshold tied to the stationary growth phase is more analogous to the −18 °C temperature threshold for microbial growth and propagation (Rummel et al., 2014) than to the −33 °C and − 40 °C thresholds for cell maintenance and survival.

For vein diameter, we adopted a threshold of $d_r > 1$ μm, which allows for full immersion and movement of psychrophilic bacteria considered relevant for Lake Vostok ice by Price (2000) and the many other bacteria species and mitochondria of comparable size and smaller. This threshold is also conservative, because the requirement of fully immersing micron-

scale bacteria in liquid veins supported by the soil pore structure is substantially more stringent than the scenario hypothesized by Rivkina et al. (2000) in which the bacterial cells themselves maintain nanometer-scale films on their surface in a manner directly analogous to small soil grains. We evaluated the S_l and d_r thresholds independently from one another, as their relationship is specific to a given soil pore geometry (see Section 4.3). We also note that future laboratory and field studies are likely to modify our S_l and d_r thresholds, just as T and a_w thresholds have been adjusted over time.

Building on the inference by Rivkina et al. (2000) that narrowing of liquid films and veins at low temperature inhibited metabolism by restricting nutrient transport, we hypothesized that critical S_l and d_r thresholds for nutrient transport might occur at different temperatures on Mars (where past and current habitability are unknown) relative to the Antarctic Dry Valleys (where extreme cold restricts habitability, but biomass and limited metabolism have been observed; e.g., Tamppari et al., 2012). Specifically, we anticipated that abundant perchlorates within Martian soils could level the habitability playing field as compared to relatively perchlorate-poor Antarctic soils, compensating for the ~50 °C temperature difference between these two environments.

Two existing sets of soil characterization data allowed us to test this hypothesis. First, Sizemore and Mellon (2008) extensively characterized soils collected at three sites in Beacon Valley, Antarctica, documenting the range of their porosities, intrinsic grain densities, permeabilities, diffusive properties, grain sizes, and pore size distributions. Chen et al. (2020) later used mercury porosimetry data from the same Beacon Valley soil samples (Sizemore and Mellon, 2008) to validate techniques for predictive modeling of residual liquid in porous media. These Beacon soil samples have been studied as Mars analogs, and they are broadly representative of sand-dominated soils in the Dry Valleys region, which are derived from local weathering of Beacon Sandstone and Ferrar Dolerite bedrock. Second, soils at the Phoenix landing site were imaged by the optical and atomic force microscopes, allowing Pike et al. (2011) to develop particle size distributions indicating that Phoenix soils are silty sands. Orbital and in situ thermal data have also been used to constrain the porosity of soils at the Phoenix site (Zent et al., 2010). These in situ constraints on the characteristics of the Phoenix soils are sufficiently detailed for predictive modeling of residual water content following the approach of Chen et al. (2020).

We have treated the Beacon and Phoenix particle size distributions as representative "Antarctic" and "Martian" soils. Additionally, we chose magnesium perchlorate, $Mg(ClO_4)_2$, and sodium chloride, NaCl, as approximate eutectic endmembers for the range of naturally occurring salts on Earth and Mars (Table 1). We then investigated the freezing behavior of both soils in salt-free, high-eutectic solute, and low-eutectic solute scenarios under appropriate environmental conditions.

3. Methods

To examine the unfrozen water fraction and refugia diameter in the Martian environment, we integrated models of climate and permafrost temperature cycles with synthetic soil freezing curves (SFCs) to calculate the time evolution of ice vs liquid water content in the permafrost over the past 2.5 Myr of Martian orbital history. We also combined our SFCs with soil and ice temperature data measured in situ in the Antarctic Dry Valleys, specifically focusing on ice temperature data collected in University Valley, Antarctica, the highest-elevation, coldest Dry Valley, most analogous to Mars and most challenging to life (e.g., Kounaves et al., 2010; Tamppari et al., 2012; Marinova et al., 2013; Marinova et al., 2022). We then compared the results of these calculations to the limits of the habitable conditions for both S_l and d_r. Finally, we compare where the limits of habitable S_l and d_r fall relative to the conventional habitability criteria for T and a_w (discussed above) for each environment.

3.1. Monte Carlo simulations of soil freezing

We have combined laboratory data and numerical simulations of soil freezing to produce best-approximation SFCs for soils with the grain size distribution and porosity observed at the Phoenix landing site (Pike et al., 2011) and collected in Beacon Valley, Antarctica (Sizemore and Mellon, 2008). Our methods build on the combined empirical-algebraic approach of Sizemore et al. (2015), the Monte Carlo modeling techniques of Chen et al. (2020), and the laboratory NMR measurements of Lei et al. (2022).

Fig. 2 shows log-normal fits to particle size distributions based on in situ microscopic imaging of the Phoenix soil (a sandy silt; Pike et al., 2011) and laboratory characterization of Beacon Valley soil samples (moderately coarse sands; Sizemore and Mellon, 2008). Following Chen et al. (2020), we used a "drop-and-roll" algorithm to generate synthetic soil packings containing 400,000 particles drawn from these distributions, and we sampled the resulting media at 10,000 random locations distributed throughout each of 100 circular planar regions of radius 200 times the median particle diameter. Using the constraints imposed by

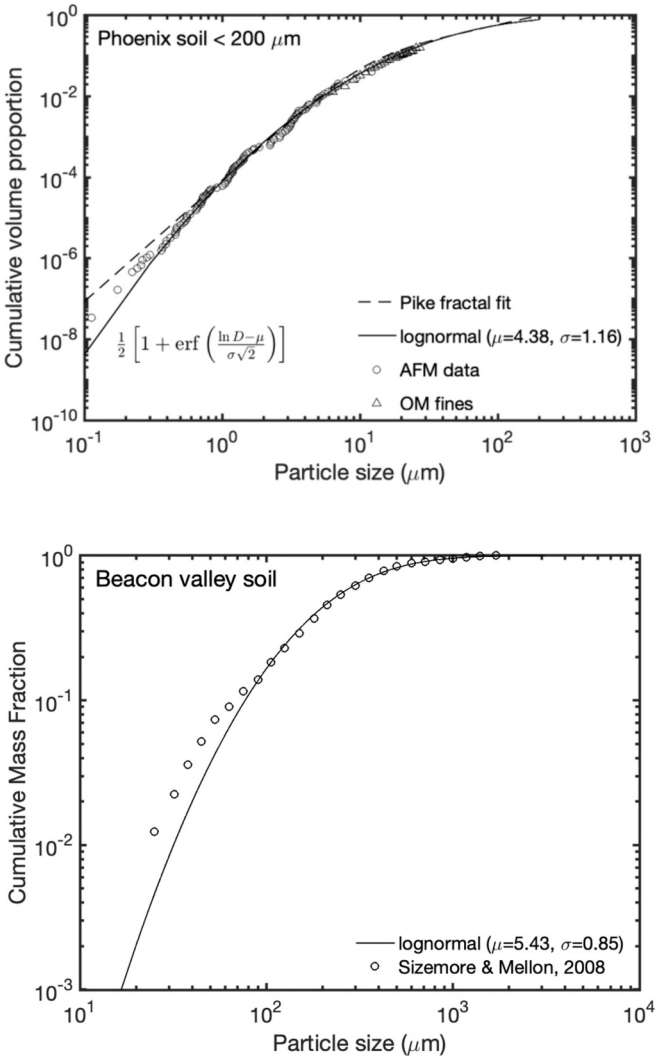


Fig. 2. Log-normal fits to the measured particle size distributions of soils at the Phoenix landing site (top) and in Beacon Valley, Antarctica (bottom). The Phoenix grain size distribution is shown here as a cumulative volume fraction, reflecting its determination from optical microscope (OM) and atomic force microscope (AFM) images (Pike et al., 2011). The Beacon grain size distribution is shown as cumulative mass fraction, consistent with its determination via dry sieving (Sizemore and Mellon, 2008).

the nearest particle surfaces, we applied the geometrical analysis of Chen et al. (2020) to evaluate both the local melting temperature at each sample point and the diameter of the largest associated liquid refugia, d_r. The pale grey lines in Fig. 3 approximate the dependence of liquid saturation on sub-zero temperature in each of the individual planar regions to illustrate the scale of anticipated heterogeneity in phase behavior that arises from the spread in particle sizes (gauged by the standard deviation of the logarithm in particle diameter, σ, as noted on Fig. 2) when interfacial films are neglected so that all residual liquid is attributed to the Gibbs-Thomson effect, using an ice-liquid surface energy of 0.029 J/m^2 (Hardy, 1977). The black lines in Fig. 3 show the SFCs constructed from the Monte Carlo model at all 10^6 sampled points, with the different dashed lines incorporating the contributions from interfacial films using the different assumed thickness behaviors indicated in the legend. The effects of salt doping for these cases are illustrated with colored lines. We considered two salt species, NaCl and Mg

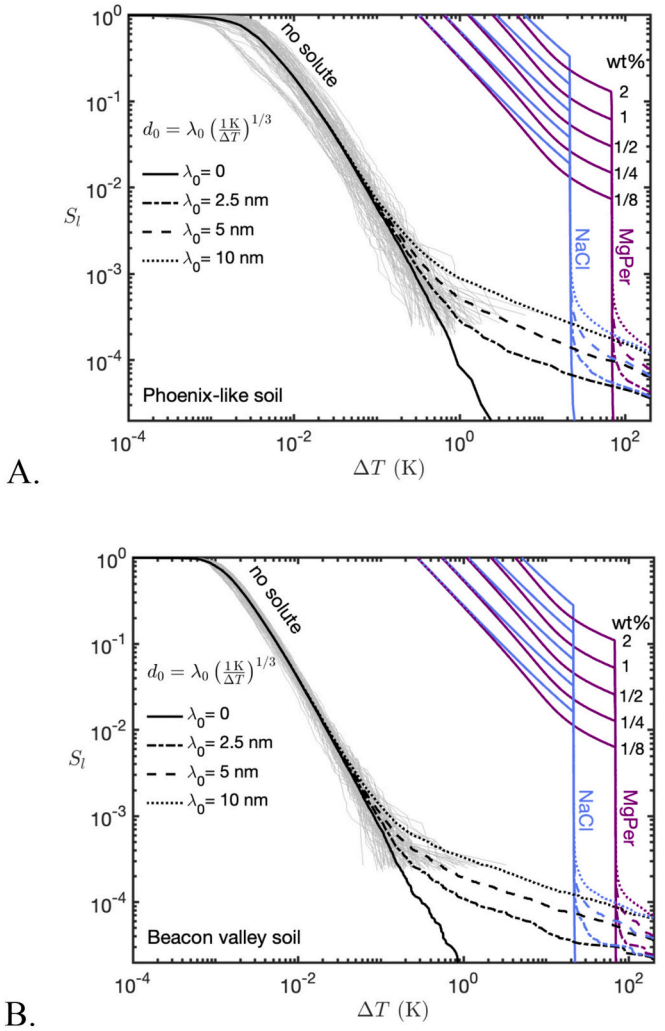


Fig. 3. Model SFCs for our example "Martian" and "Antarctic" soils, displayed as $S_l(DT)$, where DT is °C below freezing, "undercooling". Pale grey lines represent Monte Carlo sampling of the pore space of 3D synthetic soils across many differently orient 2D planes for salt-free simulations. Black lines represent the combination of all planes for the salt free case. Dashed lines represent the combined result for different assumptions of liquid film thickness in the zero-curvature case (i.e., a flat interface between the ice and mineral substrate). The purple and blue curves represent modification of the SFCs by the addition of 1/8, ¼, ½, 1, and 2 dry wt% NaCl and $Mg(ClO_4)_2$ respectively. Note that S_l is discussed in the text as a percentage and indicated here as a fraction, i.e. $S_l = 0.1 = 10$ %. (For interpretation of the references to colour in this figure legend, the reader is referred to the web version of this article.)

$(ClO_4)_2$, as endmember examples of salts that weakly and strongly reduce the freezing temperature.

3.2. Dynamic simulations of permafrost liquid fraction

We investigated the concurrent variability of temperature, T, water activity, a_w, pore-space liquid fraction, S_l, and maximum liquid vein diameter, d_r, in both the Martian and Antarctic Dry Valley environments. For the Martian environment, we employed two numerical models, a standard Mars-thermal and ice-stability model (hereafter, the "climate model"; described in detail by Mellon and Sizemore, 2022) and a Martian frost heave model (described by Sizemore et al., 2015; hereafter, the "liquid fraction model"). Briefly, the climate model (Mellon and Sizemore, 2022; Mellon et al., 2024) combines three components, including (1) a finite difference solution to the thermal diffusion equation to solve for soil temperatures as a function of time and depth (Mellon and Jakosky, 1993; Mellon et al., 2000), (2) a tuned climate model to determine near-surface water vapor content as a function of obliquity, latitude, soil properties, and elevation (Jakosky et al., 1993; Mellon and Phillips, 2001; Mellon and Sizemore, 2022), and (3) an iterative convergence approach to determine the depth of the ice table in a given epoch assuming diffusive equilibrium with atmospheric water vapor (e.g. Mellon et al., 2004). These model components have been used extensively to examine the distribution and dynamics of icy permafrost and thermal emission/thermal inertia, and they represent the current state-of-the art in terms of historical simulation of ice-table depth and temperature. We previously included the computation of water activity of the ice-rich permafrost at and below the ice table (Mellon et al., 2024); in the current work, we further augmented this approach with calculations of S_l and d_r, based on our newly developed SFCs describing $S_l(T)$ and $d_r(T)$ for specific soil types and salt doping.

We employed the liquid fraction model (Sizemore et al., 2015) to calculate the habitability conditions in targeted portions of parameter space. The liquid fraction model uses initial and surface boundary conditions provided by the climate model to recalculate T, a_w, S_l, and d_r in the icy permafrost based on a modified thermal diffusion equation, which includes a latent heat term and accounts for the variability of the thermal conductivity and specific heat capacity of the ice-cemented soil due to changes in S_l. Significant temperature differences ($|DT| > 1.5$ °C) did not arise between the climate model and liquid fraction model for $T_{max} < 263$ K (−10 °C), much warmer than temperatures experienced by the Martian ice table in the past several Ma. Thus, this secondary set of simulations served as a targeted check of the simpler calculation based on the climate model alone.

We employed our combined climate and liquid fraction model to calculate maximum values of all four habitability conditions (T, a_w, S_l, and d_r) over 2.5 Ma of Mars climate history and latitudes from 30°-70°N. We used the thin film model to predict summertime diurnal variability of all parameters under recent climate conditions previously identified as favorable to life (i.e., 70° N, 630 ka before present, obliquity = 34.7°, see Mellon et al., 2024) and under present-day climate conditions at the same latitude, which are generally considered unfavorable to life. In these diurnal simulations we investigated salt-free and 1 dry wt% magnesium perchlorate doping scenarios for both soil types.

Finally, we calculated a_w, S_l, and d_r for ice-cemented ground in University Valley, Antarctica directly from ice temperature data measured over a full seasonal cycle by Marinova et al. (2022). The Dry Valleys of Antarctica have been studied extensively as analogs to the Martian northern plains, due to the presence of dry permafrost (ground that never warms above 0 °C and has negligible ice content) occurring above ice-cemented soil. University Valley and adjoined Beacon Valley have received particular attention, as their high-elevation, inland location produces the coldest and driest Antarctic conditions most analogous to Mars (e.g., McKay et al., 1998; Kounaves et al., 2010; Tamppari et al., 2012; Marinova et al., 2013, 2022). University Valley is a small hanging valley adjacent to the larger, and nominally lower-elevation Beacon

Valley. The Antarctic soil samples on which we based our Monte Carlo soil-freezing simulations were collected in Beacon Valley (Sizemore and Mellon, 2008), but are also typical of University Valley soils and the unconsolidated soils of the Dry Valleys region more generally. As such, we refer to the soil freezing curves generated from the Beacon samples as "Antarctic" or "Beacon" SFCs, interchangeably. In calculating habitability parameters for an Antarctic environment, we specifically used environmental data from University Valley as representative of "Antarctic" climate conditions. We intentionally neglected lower altitude, more coastal valleys in which temperatures can seasonally exceed 0 °C, bulk melting periodically occurs, and temperature is not a dominant restriction for life. We applied only the Beacon SFCs and refugia data to our investigation of the Antarctic environment. We considered salt-free, NaCl-doped, and $Mg(ClO_4)_2$-doped cases, to capture endmember and intermediate behavior. Many other soluble salts are common in the Dry Valleys and on Mars (e.g., chlorides and nitrates; see Table 1 and Discussion).

We emphasize that in all these scenarios, we considered the habitability of ice-and-liquid saturated permafrost below the ice table only; we explicitly neglected the overlying dry permafrost (in the Martian & Antarctic cases) and dry active layer (in the Antarctic case). As such, we assumed that liquid films and veins were always in thermodynamic equilibrium with pore ice, such that $a_w = P_{H2O(cr)}/P_l$, where $P_{H2O(cr)}$ is the water vapor pressure over ice at temperature T and P_l is the vapor pressure over pure liquid water at the same temperature, making water activity, a_w, a simple function of ice temperature. This treatment reproduces our earlier procedure (Mellon et al., 2024), consistent with Murphy and Koop (2005), Tosca et al. (2008), and others.

4. Results

4.1. Soil Freezing Curves (SFCs)

Fig. 3 shows the new model SFCs for our example Phoenix and Beacon soils. The SFCs for both soil types share a few noteworthy characteristics. First, for both soils the salt-free cases (black lines) are well approximated by power law fits for $T \lesssim -0.1\,^{\circ}$C (c.f., Sizemore et al., 2015; Chen et al., 2020). Variation from the power law at lower T (larger undercooling, ΔT) depends on our assumption of the thickness of a premelted film at a flat interface, λ_o. (Note that λ_o is the thickness of the interfacial film represented schematically in Fig. 1, while d_r is diameter of the much larger liquid veins near mineral grain contacts.) The assumed value of λ_o makes only a minor contribution to S_l ($\sim 10^{-4} = 0.01$ % to $10^{-3} = 0.1$ %), preferentially at low temperature. Fig. 3 shows a range of reasonable choices for λ_o (Chen et al., 2020), which may be somewhat conservative in terms of low-temperature liquid

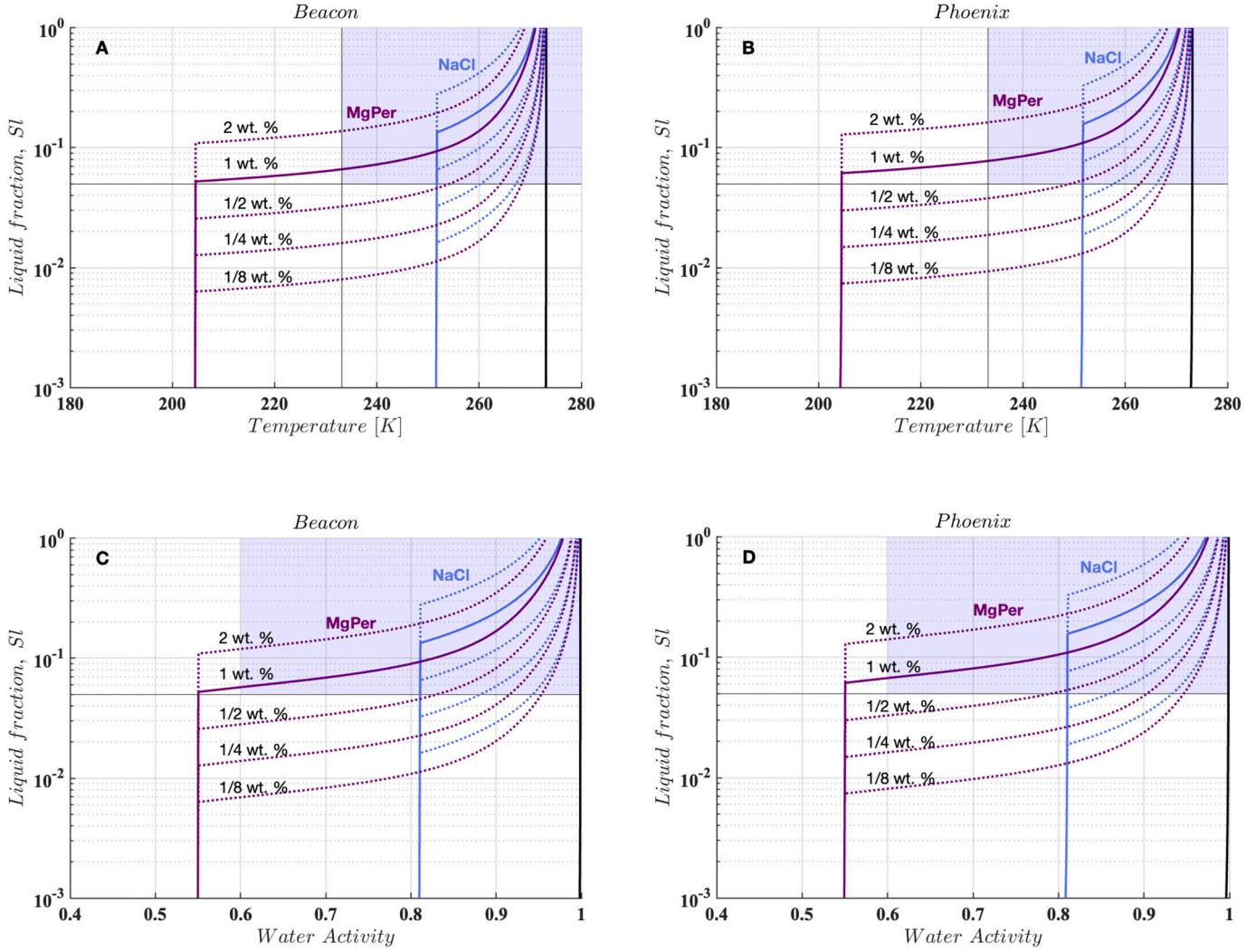


Fig. 4. Model SFCs show as functions of T and a_w. Blue boxes indicate habitability limits as defined in the current work and by Mellon et al. (2024): $T > -40$ °C, $a_w > 0.6$, $S_l > 5$ %. In all cases shown here, $\lambda_o = 0$ nm. Note that S_l is discussed in the text as a percentage and indicated here as a fraction, i.e. $S_l = 0.1 = 10$ %. (For interpretation of the references to colour in this figure legend, the reader is referred to the web version of this article.)

availability and habitability (Lei et al., 2022). For calculations in subsequent sections, we assumed $\lambda_o = 10$ *nm*. A factor of ~3 difference in the salt-free SFCs is apparent between the Phoenix and Beacon soils, where the greater fine-grain component of the silt-dominated Phoenix soil generally produces more residual liquid relative to the coarser Beacon sand at an equivalent temperature. The addition of salts (blue and purple lines) reveals a second broad similarity between the soil types: With solutes in the system, SFCs for each soil are elevated and shifted to lower temperatures (greater undercooling), but retain their shape above the eutectic (note the right-ward shift in Fig. 3 corresponds to a leftward shift in Fig. 4, discussed below), resulting in liquid fractions of a few to several percent at temperatures significantly below the bulk freezing temperature of pure water for the 1 wt% doping cases (consistent with both Sizemore et al., 2015 and Chen et al., 2020). In all salty cases, S_l drops abruptly to the salt-free value below the eutectic temperature, with our assumption of λ_o again introducing minor variability in the smoothness of this transition at low temperature.

An additional feature to note in Fig. 3 is that the total freezing point depression for the salty cases (T_f, the temperature at which ice first infiltrates the pore space) combines the freezing point depression due to confinement effects alone ($S_l = 1$, black curves) with the freezing point depression due to colligative effects, which depends upon both salt species and concentration. We have made the somewhat arbitrary choice of focusing our parameter studies (sections 4.3 and 4.4) on salt concentrations of 1 dry wt%, loosely consistent with the concentration of perchlorates inferred in soils at the Phoenix landing site (Kounaves et al., 2014; Toner et al., 2014a). We calculated SFCs for concentrations of both salts ranging from 1/8 to 2 dry wt%. Because we have defined salt concentrations based on dry weight, the freezing point depression for our sodium chloride examples is slightly greater than that of our magnesium perchlorate examples, because we are effectively considering a smaller molar concentration of magnesium perchlorate relative to NaCl, due to the large mass of the $Mg(ClO_4)_2$ molecule. This difference illustrates that key details of SFCs depend on the specific solutes present and their local concentration – and this may have important implications for liquid availability and habitability at a specific location or soil horizon on Earth or Mars. At the same time, the broad characteristics of freezing in a porous medium as reflected in Figs. 2 and 3 are fairly universal (e.g., Chen et al., 2020).

Fig. 4 shows the SFCs replotted as $S_l(T)$ and $S_l(a_w)$ for easy comparison to the habitability thresholds outlined in our previous paper (Mellon et al., 2024). The key difference among our current modeled cases is that the eutectic temperatures of our example salts (NaCl, −21 °C or 252 K; $Mg(ClO_4)_2$, ~ − 67 °C or 206 K) and the no-salt scenarios result in dramatically different liquid availability at Mars-relevant temperatures. When magnesium perchlorate is present at Phoenix-like concentrations in either soil (1 dry wt%), our $S_l > 5$ % habitability requirement is met down to temperatures well below the extreme low temperature limit of −40 °C (233*K*). In the Phoenix-like soil, S_l doesn't drop below 5 % until a water activity of 0.55, below the cut-off of 0.6. In the Beacon soil, the 1 wt% $Mg(ClO_4)_2$ curve crosses the $S_l > 5$ % threshold near $a_w = 0.6$, but as in the Phoenix case, remains relatively flat until reaching the eutectic temperature and $a_w \sim 0.55$.

Without salts, pore-confinement effects do little to extend the range of habitable S_l relative to T or a_w for either soil. Bulk freezing point depression in both cases is less than 1 °C and S_l falls below 5 % for $a_w >$ 0.98. Although these scenarios are more favorable to habitability below 0 °C (273 K) than pure, soil-free ice, they offer no substantial advantage in terms of Martian or Antarctic liquid availability. This underscores the fact that very salt-poor permafrost may have minimal residual liquid at temperatures only a few degrees below bulk freezing, which could constitute a major impediment to nutrient and waste transport, and thus habitability.

Our 1 wt% NaCl cases illustrate an intermediate scenario. Above the NaCl eutectic ($T > -21$ °C), S_l is larger in the case of NaCl than for $Mg(ClO_4)_2$ at an equivalent temperature, exceeding 10 % for $T > -21$ °C, $a_w > 0.8$. However, for NaCl, S_l drops sharply to <0.1 % at a temperature just below the "propagation limit" of −18 °C and well above the nominal metabolic limit of −33 °C (see also Rummel et al., 2014).

These examples are instructive in that they allow us to consider how a wide variety of single-salt species SFCs might cross the boundaries of our habitability limits. The lower concentration cases of both salts species produce SFCs that exceeded $S_l = 5$ % for a more restricted range of temperatures and water activities than the 1 wt% case. Conversely, the 2 wt% cases increase the value of S_l (and presumably the efficiency of nutrient transport) for a given temperature above the eutectic, but do not extend elevated values of S_l beyond the defined range of "habitable" T and a_w. However, the most realistic scenario on the ground is one in which multiple salt species contribute to residual liquid across and below the currently defined range of habitable temperatures, with the individual eutectic temperatures introducing a stepped structure to the SFC, and the individual salt concentrations determining the temperature at which the 5 % threshold is crossed.

4.2. Refugia diameter

Results from our investigation of maximum liquid vein diameter, or refugia diameter, d_r, have similar implications. Fig. 5 shows liquid fraction as a function of d_r for the "Martian" and "Antarctic" particle size distributions, respectively. Note that these relationships are purely functions of the soil pore geometry and are temperature and salt-content independent. The curves have a broadly similar shape, but they are offset from one another. For a given liquid fraction the Antarctic soil typically contains larger liquid veins due to its relative lack of fine particles. Note that this does not contradict our earlier observation that the salt-free Martian soil contains more liquid than the salt-free Antarctic soil *at an equivalent temperature*. The greater abundance of silt-sized particles in the Martian soil provides more locations at which the Gibbs-Thomson effect can produce residual liquid, but simultaneously restricts the size of the soil pores and liquid veins. Conversely, the larger particles in the Antarctic soil offer fewer sites for liquid veins to form in an equivalent volume of soil, but simultaneously allow for the development of larger individual veins.

To determine the variation of d_r with T, we must combine each of our SFCs with the refugia curve for the corresponding soil geometry. Fig. 6 shows $d_r(T)$ for all six scenarios (Martian and Antarctic particle size distributions; salt-free, NaCl, and $Mg(ClO_4)_2$ 1 dry wt% cases). For a given temperature, both salts increase the maximum vein diameter substantially. Without salts, d_r drops to <1 μm above $T = -3$ °C. In salt-

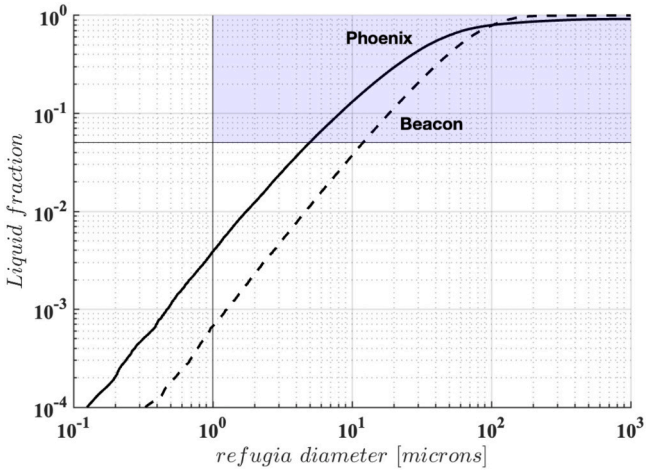


Fig. 5. Liquid fraction, S_l, as a function of maximum vein diameter, d_r, for the Beacon soil (dashed line) and the Phoenix soil (solid line). Note that S_l is discussed in the text as a percentage and indicated here as a fraction, i.e. $S_l = 0.1 = 10$ %.

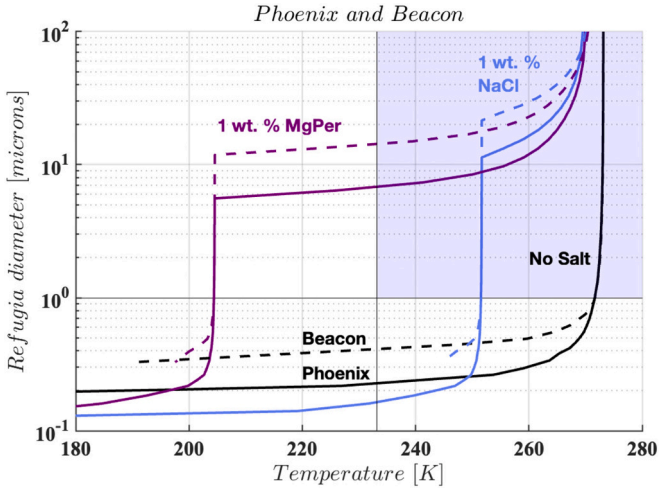


Fig. 6. Refugia diameter, d_r, as a function of T for the Beacon (dashed lines) and Phoenix (solid lines) soils, with no salt (black), 1 dry wt% NaCl (blue lines), and 1 dry wt% $Mg(ClO_4)_2$ (purple lines). (For interpretation of the references to colour in this figure legend, the reader is referred to the web version of this article.)

free cases, small veins will constitute a challenge to physical accommodation or immersion of single celled organisms, vein network connectedness, and nutrient-waste transport in both the Martian and Antarctic environments. Conversely, in the salty cases the largest pores are typically several microns to >10 μm in diameter, allowing for full immersion and possible movement of micron-scale cells. The combination of multi-micron scale veins (Fig. 6) and $S_l > 5$ % (Fig. 5) suggest that liquid vein networks are adequately connected for transport of nutrients and waste at all temperatures above the eutectic for both salts and both soil geometries. Broadly, this leads us to conclude that meeting the requirement of $d_r > 1$ μm is surprisingly easy for silty to sandy soils with plausible salt doping. Two factors could limit the occurrence of these large liquid veins in the Martian and Antarctic Dry Valleys environments: (1) a major deficit of salts, and/or (2) soils with abundant clay-sized particles.

4.3. Application to the historical Martian habitat

Applying the results of sections 4.1–4.2 to recent Martian climate history yields a surprising picture of liquid availability in the shallow ice-rich regolith. Fig. 7 shows contour plots of the seasonal maximum pore space liquid fraction and refugia diameter occurring in a Phoenix-like soil containing 1 wt% $Mg(ClO_4)_2$ between 30°N and 70°N latitude over the past 600 kyr of Martian climate history. This parameter space corresponds to the ice-stability history we calculated in our previous paper (Mellon et al., 2024), indicating that abundant ground ice likely

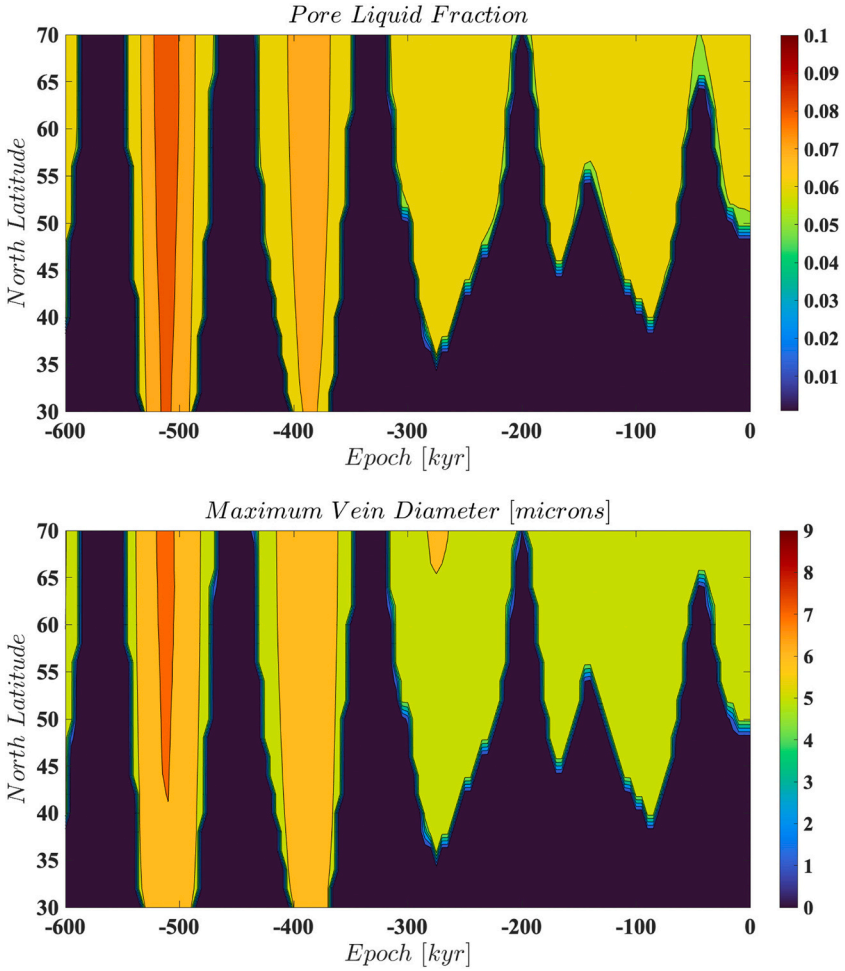


Fig. 7. Maximum values of S_l (top) and d_r (bottom) in the Phoenix soil with 1 dry wt% $Mg(ClO_4)_2$ over the past 600 thousand Martian years poleward of 30°N. Note that habitability criteria are met repeatedly during this time period due to high-obliquity excursions; earlier, higher obliquity excursions produced higher values of S_l and d_r for longer time periods. S_l is discussed in the text as a percentage and indicated here as a fraction, i.e. $S_l = 0.1 = 10$ %.

occurred at these times and latitudes. Recent high obliquity excursions have produced multiple relatively "clement" periods during which the liquid content of the ice-filled pore space likely approached 10 % and the largest liquid veins in the soil-ice cement were several microns in diameter at all latitudes poleward of 30° N. Further, our simulations indicate that for Phoenix-like soils poleward of 50°N, 1 wt% $Mg(ClO_4)_2$ produces $S_l \sim 6$ % and $d_r > 5$ μm *in the current climate*, whereas ground ice itself is predicted to be currently stable poleward of ~47°N (Mellon et al., 2024). However, between 50°N and 47°N the depth of the ground ice increases such that seasonal ice temperatures are insufficiently warm to raise S_l and d_r to habitable limits.

The present-day values of S_l and d_r would drop below our habitability thresholds if we assumed a lower concentration of magnesium perchlorate (in some locations more consistent with in situ data; see summary in Rzymski et al., 2024). However, the wide-spread availability of many salt species on Mars, combined with our simulations suggests that liquid availability may not be the limiting factor for habitability even under current, extremely cold conditions. Although perchlorate concentrations in some consolidated Martian rock strata fall below detection limits (Stern et al., 2017; Archer et al., 2024) concentrations >0.2 wt% are more typical in unconsolidated soils and aeolian materials at most landing sites (Rzymski et al., 2024).Thus, S_l and d_r are unlikely to have been the limiting factors for Martian permafrost habitability over the past 2.5 Ma, despite seasonal peak ice temperatures typically not exceeding −33 °C. The many obliquity excursions that produced relatively "clement" ice temperatures also had the potential to produce liquid vein networks that exceed our habitability criteria (Fig. 7).

To contrast the current epoch with a recent "more habitable" epoch (630 kyrs ago) in more detail, we examined the summertime diurnal variability of all four habitability metrics (T, a_w, S_l, d_r) for both soil geometries, with and without $Mg(ClO_4)_2$. Table 2 shows maximum and minimum values of all parameters for a 10-sol mid-summer period beginning at Ls = 100° at 70°N latitude in the current epoch (0 ka; obliquity = 25°) and the relatively clement period at −630 ka (obliquity = 34.7°) in the Laskar et al. (2004) orbit history. The effects of grain size on total liquid fraction and maximum vein diameter are somewhat complicated, because grain size not only plays a role in the geometry of the residual wetting phase below the ice table, it also affects the thermal inertia of the dry soil layer above the ice table (Table 3), and thus the ice-table depth and peak temperatures. During the high-obliquity "clement" period 630 thousand years ago, our simulations indicate summertime shallow ice temperatures were above the nominal metabolic limit of $T \geq -33$ °C (Rummel et al., 2014; Mellon et al., 2024) in both soil types, and a_w was correspondingly high. Under these conditions, the addition of $Mg(ClO_4)_2$ raises S_l to ~7–8 % and d_r to 7–15 μm, comfortably exceeding habitability thresholds for both soils. However, in the absence of salts, $S_l = 0.03$ % in the Phoenix soil and $S_l = 0.3$ % in the Beacon soil, indicating the network of liquid veins, although present, is poorly connected – even in the Beacon case, where larger grains and pores nominally allow $d_r > 1$ μm. In the context of transport limits observed by Ostroumov and Siegert (1996) and Rivkina et al. (2000), our results indicate that S_l is a critical bottleneck in "warm" salt-poor settings. Conversely, in the current Martian climate, adequate concentrations of $Mg(ClO_4)_2$ could allow the Phoenix soil to maintain a robust vein network ($S_l \sim 6$ %, $d_r \sim 6$ μm). The total liquid fraction remains a restriction in the perchlorate-doped Beacon soil, with $S_l < 1$ %. The salt-free scenarios in the current Martian climate are universally unfavorable.

4.4. Application to the Antarctic Dry Valleys habitat

We focused our analysis of the Antarctic environment on a meteorological station in University Valley (77°51.729′S, 160°42.606′E, elevation 1677 m) at a location with an ice-table depth of 42 cm (Marinova et al., 2022). As noted previously, our "Antarctic" soil freezing and refugia curves are derived from soil samples collected in the adjoining Beacon Valley; both locations exhibit sand-dominated particle-size distributions, as these soils are derived from local weathering of the same Beacon Sandstone and Ferrar Dolerite bedrock.

Fig. 8 shows the ice table temperature over one seasonal cycle at this location and the corresponding values of S_l and d_r calculated for the Beacon soil geometry. Ice temperatures are perennially above the extreme metabolic limit of −40 °C (Mellon et al., 2024). As in the Martian cases, however, liquid availability is critically dependent upon salts. At the 1 dry wt% concentrations we modeled, both salt species produce $S_l \geq 10$ % and $d_r > 10$ μm during the Antarctic summer; additionally, $Mg(ClO_4)_2$ allows $S_l \sim 8$ % and $d_r > 10$ μm to persist through the winter months. Notably, S_l and d_r never meet our habitability criteria

Table 2
Summary of maximum and minimum values of T, a_w, S_l, and d_r in 10-sol simulations starting at aerocentric longitude of perihelion $L_s = 100°$ and 70° N latitude during the recent high obliquity excursion at −630 ka in the Laskar et al. (2004) orbit history and in the current Martian climate. Note that S_l is discussed in the text as a percentage and indicated here as a fraction, i.e. $S_l = 0.1 = 10$ %.

70° N, −630 ka											
Soil Type		Ice table T [K]		Ice table T [°C]		Water Activity		Liquid Fraction		Refugia Diameter [mm]	
		max	min	max	min	max	min	max	min	max	min
Phoenix	salt free	241.2	234.7	−31.95	−38.45	0.73	0.69	3.10E-04	2.85E-04	0.241	0.231
	Mg perchlorate	241.2	234.3	−31.95	−38.85	0.73	0.69	0.087	0.081	7.35	6.95
Beacon	salt free	241	234.3	−32.15	−38.85	0.73	0.69	0.0033	0.003	2.47	2.33
	Mg perchlorate	241	234.4	−32.15	−38.75	0.73	0.69	0.074	0.068	15.24	14.47

70° N, 0 ka											
Soil Type		Ice table T [K]		Ice table T [°C]		Water Activity		Liquid Fraction		Refugia Diameter [mm]	
		max	min	max	min	max	min	max	min	max	min
Phoenix	salt free	209.8	204.2	−63.35	−68.95	0.57	0.55	2.32E-04	2.24E-04	0.209	0.207
	Mg perchlorate	209.9	205.2	−63.25	−67.95	0.57	0.55	0.063	0.063	5.78	5.61
Beacon	salt free	209.3	203.8	−63.85	−69.35	0.57	0.55	1.00E-04	1.00E-04	0.328	0.328
	Mg perchlorate	209.3	203.8	−63.85	−69.35	0.57	0.55	0.0023	0.0022	2.01	1.96
Thresholds											
propogation limit		≥ −18 °C		≥ 255.15 K							
nominal metabolic limit		≥ −33 °C		≥ 250.15 K		≥ 0.6		≥ 0.05		≥ 1	
extreme metabolic limit		≥ −40 °C		≥ 233.15 K							

Table 3
Dry soil thermal properties for Martian setting.

Soil Geometry		Dry Permafrost				Icy Permafrost			
	Porosity	k	r	c	I	k	r	c	I
Phoenix	0.55	0.078	1652	619	282	2.65	2160	1159	2575
Beacon	0.41	0.039	1630	850	232	2.5	2009	1158	2411

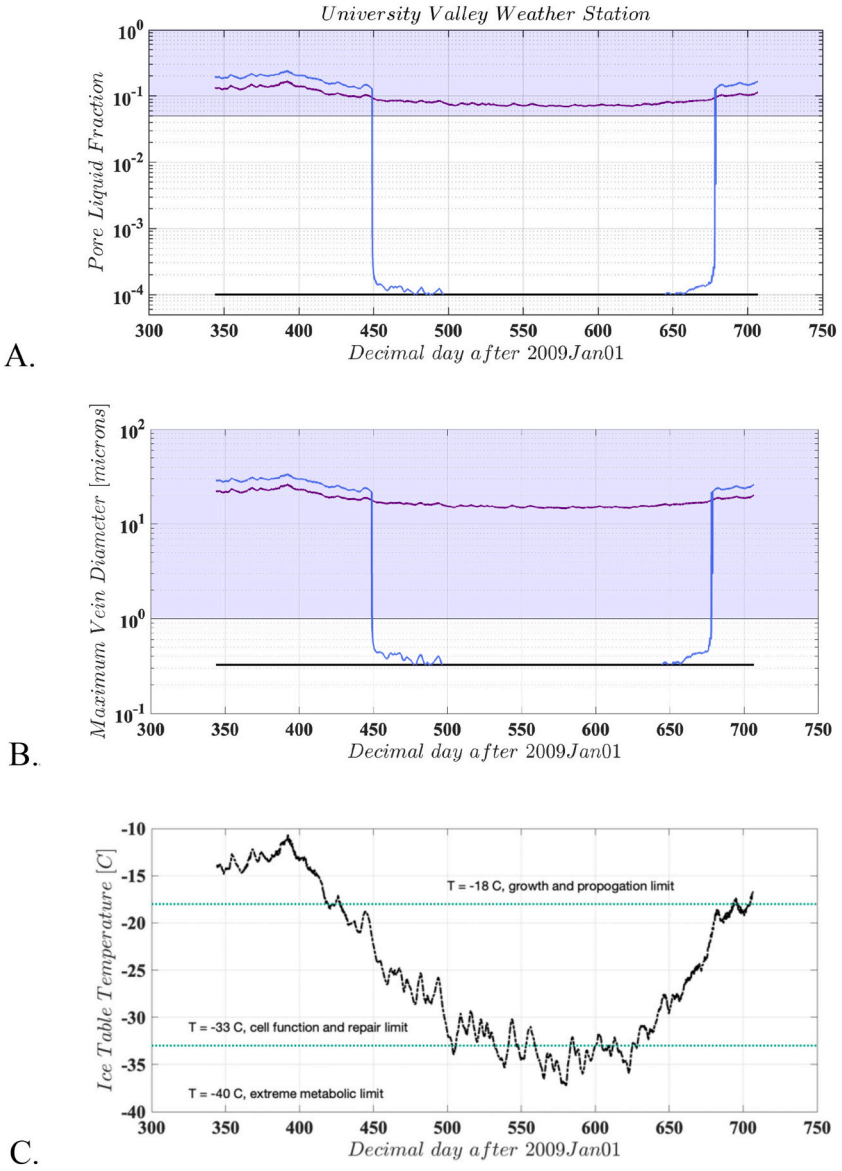


Fig. 8. S_l (a) and d_r (b) at the ice table in University Valley calculated for the Beacon Valley soil with no salt (black), 1 dry wt% NaCl (blue), and 1 dry wt% $Mg(ClO_4)_2$ (purple), based on one seasonal cycle of temperatures measured in situ (c). Blue shaded regions indicate habitability criteria are met in (a) and (b). Three temperature thresholds for habitability are indicated by green lines in (c). Note that the salt-free scenario never meets either habitability criterion ($S_l > 5$ %, $d_r > 1$ μm), despite temperatures that perennially exceed the extreme metabolic limit of −40 °C. S_l is discussed in the text as a percentage and indicated here as a fraction, i.e. $S_l = 0.1 = 10$ %. (For interpretation of the references to colour in this figure legend, the reader is referred to the web version of this article.)

in the salt-free case, and both parameters drop below habitability thresholds during the winter months in the NaCl case.

None of the three salt-content scenarios illustrated in Fig. 8 are strictly representative of the solutes present in University Valley, but they constrain our understanding of residual liquid there. Table 1 shows a variety of naturally occurring salts and acids that could plausibly contribute to residual liquid in both Martian and Antarctic permafrost environments. Field work has constrained the relative abundances of some solutes in University Valley, based on ion chromatography (Kounaves et al., 2010; Tamppari et al., 2012). Perchlorates are present in University Valley at some of the highest natural concentrations on Earth (~30–600 mg/kg or 30-600 × 10^{-10} wt%; Kounaves et al., 2010), but far below Martian levels (~6 g/kg or 0.6 wt%; Kounaves et al., 2014), and likely do not allow for significant residual liquid in winter or contribute significantly to S_l in summer. Chlorides and nitrates, conversely, are abundant in the Dry Valleys (~0.01–0.2 dry wt% and ~

0.01–0.5 dry wt%, respectively; Kounaves et al., 2010) and their combined effect would be broadly similar to the NaCl result shown in Fig. 8, i.e. providing summertime S_l in the ~1–10 % range, with little residual liquid remaining in winter. As discussed in the Martian case, the combined effects of multiple salt species may produce a stepped behavior, with S_l above the habitable >5 % limit at the highest summertime temperatures, intermediate but potentially still habitable S_l between the eutectic temperatures of the dominant salt species during fall and spring, and near-complete wintertime freeze out.

The concentrations of specific chlorides and nitrates present at a particular University (or Beacon) Valley location will dictate the seasonal timing of when (and if) our habitability thresholds are crossed. The lowest solute concentrations measured by Kounaves et al. (2010) and Tamppari et al. (2012) raise the possibility that some Dry Valley soils are locally so salt-poor that habitable S_l and d_r never occur, even in the austral summer. Conversely, the combined effects of the highest nitrate and chloride concentrations measured by Kounaves et al. (2010) should produce S_l directly comparable to our NaCl calculation during the warmest months. In addition, unpublished measurements of the soluble-salt content of the Beacon Valley soil (M. T. Mellon) ranged from 0.5 up to 9 wt%, depending on the depth, consisting mostly of salts of nitrate, sulfate, and chloride. Further investigation of spatial variations in soluble salt concentrations is needed to determine how salt-poor or salt-rich soil horizons will produce regional deficits or enhancements in residual liquid and related conditions for habitability of the icy permafrost in the Beacon-University region.

5. Discussion

5.1. Complexities of natural environments & limitations for ground-ice habitability

Our modeling approach neglects some characteristics of soil freezing in the natural environment that are relevant to habitability, specifically: super-cooling, SFC hysteresis, non-uniform spatial distribution of solutes, and the redistribution of solutes via the liquid vein network itself. Many brines exhibit hysteresis in the freezing and thawing process – i.e., a substantial volume of supercooled liquid persists as temperature is decreased past the eutectic, but the same volume of liquid is not recovered at equivalent temperatures when the frozen brine mixture is warmed (Toner et al., 2014a; Shumway et al., 2023). This effect can produce distinct warming and cooling branches in empirical SFCs at sub-eutectic temperatures. Shumway et al. (2023) performed warming-branch experiments on regolith and perchlorate-brine samples to compensate for hysteresis, and they still observed significant supercooled liquid below the eutectic. The timescale of their observations was short (~ 15 min), so their results may not capture the behavior of the sub-eutectic liquid fraction in natural environments where extremely low temperatures persist for months. In this context, our SFCs that incorporate a sharp transition in S_l at the eutectic temperature are appropriately conservative, in that they assume negligible liquid availability at sub-eutectic temperatures.

Our calculations assume a uniform vertical distribution of solutes for both Mars and Antarctica. In contrast, field measurements show vertical variation in ion concentration at centimeter to decimeter scales in University Valley, and regionally across the geographic extent of the Dry Valleys. Tamppari et al. (2012) observed variability in all soluble ion concentrations above the ice table in both Taylor and University Valleys. On Mars, significant variation in perchlorate concentration is observed between consolidated geologic strata in both Gale and Jezero Craters (below detection limits to 1.19 wt%; Stern et al., 2017; Archer et al., 2024), but aeolian materials and unconsolidated soils have shown more consistent values at all landing sites (0.2–0.6 wt%; Rzymski et al., 2024), suggesting consistent average concentrations in the dry and icy permafrost layers that we have simulated. However, little is known about the vertical distribution of perchlorate in the soil column at the Phoenix landing site; perchlorate has not been directly measured in ice cemented ground on Mars because ice-cemented material could not be sampled. Stratigraphy in the occurrence of duricrust (salt-cemented soils) is also common in the Martian dry permafrost layer, so vertical variation in solute concentration at cm to decimeter scales is likely. In University Valley, soluble ions decreased with depth toward the ice table, where a second local peak in ion concentration occurred, co-located with a peak in biomass (Tamppari et al., 2012). It is reasonable to expect that feedbacks should exist between solute concentration, time-variable residual liquid availability, and biomass concentration that produce stratigraphy below the ice table – crudely analogous to our expectation of stratigraphy of ice concentration below the ice table on Mars (e.g., Sizemore et al., 2015). Detailed modeling of liquid content in icy permafrost that contains multiple solutes with spatially variable concentrations is outside the scope of our current work. However, this type of modeling may be valuable in attempting to understand the history of residual liquid and chemical stratigraphy at future bore-hole sites in Antarctica and on Mars.

Our current work was motivated, in part, by the hypothesis that the low-temperature freezing behavior of Martian and Antarctic soils might be distinct from one another, and that their differences might extend the range of habitability to lower temperatures on Mars relative to the Dry Valleys. Our results support this hypothesis, in the sense that ubiquitous, abundant perchlorates (> 0.75 dry wt%) in Martian soils can produce "habitable" values of S_l and d_r at, and even below, the extreme metabolic temperature threshold of −40 °C (Mellon et al., 2024). Solutes with comparably low eutectic temperatures have not been detected in sufficient concentrations in the Dry Valleys to produce a similar result. Based on our Martian simulations, if perchlorates are present in plausible quantities, vein diameters may be seasonally large enough to accommodate micron-scale cell bodies and allow waste and nutrient transport *even in the current Martian climate* for latitudes poleward of 50° N. During recent past climate excursions, the total liquid fraction in the shallow ice was higher than the present day, individual veins were larger, vein networks were more connected, and these favorable conditions extended to greater subsurface depths and lower latitudes. Other salts present in the Martian environment would have contributed to this effect, providing progressive expansion of the liquid vein network at environmental temperatures above their eutectics.

The relative deficit of perchlorates in terrestrial settings precludes the maintenance of similar liquid vein networks at the lowest temperatures in University Valley. At minimum, this imposes a strong seasonal bottleneck, as illustrated by the NaCl results in Fig. 8, despite the current ~50 °C higher average temperature relative to Mars. The spatial variability of soluble ions observed by Kounaves et al. (2010) and Tamppari et al. (2012) raises the possibility that in some locations S_l and d_r might not reach threshold values, even in the warm austral summer, due to local deficits in solute concentration. It is important to emphasize that differences between the Martian and Antarctic scenarios arise principally from the different solute species at each location, with the specific pore-space geometries of our "Phoenix" and "Beacon" soils making only minor contributions to soil freezing behavior dominated by colligative effects. We have tied our synthetic soils to in situ measurements specific to both locations, but the range of natural grain- and pore-size variability in the Antarctic Dry Valleys and across Vastitas Borealis, Mars, is much greater than the differences between the "Phoenix" and "Beacon" soil examples explored here. Thus, on Mars and in the Dry Valleys, we should expect regional and hyperlocal heterogeneity in the development of liquid vein networks, driven primarily by solute availability. Pore confinement effects will become important in cases of strong grain-size sorting. For example, a very coarse sand in a solute-poor setting might produce localized micron-scale liquid veins above a particular temperature threshold, but not produce an adequate liquid volume or a vein network connected enough for nutrient/waste transport. Conversely, a soil dominated by tightly packed clay-sized particles might maintain a significant residual liquid fraction at low temperature, but vein

diameters might not meet our criteria for housing cells or transporting nutrients efficiently.

Both of these well-sorted-soil scenarios are likely to be outliers in the context of the Martian northern plains and the high-altitude Dry Valleys, which are dominated by silty sands (e.g., McKay et al., 1998; Mellon et al., 2000). Perhaps the most surprising aspect of our results is how readily residual liquid can be maintained in these soil types under Antarctic or Martian environmental conditions. A lack of summertime residual liquid is unlikely to be the dominant restriction to habitability in either setting. The optimal ingredients for producing a robust liquid vein network at low temperature are the combination of a silty to sandy soil, with a minimal clay-sized particle component, plus multiple low-eutectic temperature salts (c.f., Chen et al., 2020). High concentrations of perchlorate in the Martian regolith suggest that summertime liquid vein networks in the icy permafrost of the Northern Plains may be comparable to (or even more developed than) vein networks in University Valley.

Perchlorates offer other advantages to putative Martian microbes, including prevention of cell damage by the formation of ice and salt crystals (Shumway et al., 2023) and provision of an electron acceptor for metabolism under anoxic conditions. Lynch et al. (2019) demonstrated active perchlorate reduction by microbes in the Pilot Valley paleolake basin of Utah, a Mars analog environment where sediments are naturally enriched in perchlorate. Kounaves et al. (2010) hypothesized that the lack of perchlorate accumulation in Earth's oceans and ground water might be attributable to microbial conversion of perchlorate to chloride in low nitrate and anaerobic zones. Conversely, the abundance of perchlorate on Mars, as well as high levels of chlorate and perchlorate relative to nitrate has been interpreted to indicate distinct formation mechanisms on Mars relative to Earth, as well as a global lack of biologic activity (Stern et al., 2017).

For icy permafrost in thermodynamic equilibrium, the water activity of the liquid veins necessarily matches the water activity of the adjacent pore ice. This balance occurs independent of the presence of specific solutes that might increase or decrease the volume of residual water at a specific temperature, but it controls the concentration of a given solute in the residual liquid. The commonly established threshold for habitability based on a water activity is 0.6, as lower water activity may result in denaturization (see Rummel et al., 2014 and references therein). In equilibrium with ice $a_w = 0.6$ would correspond to a temperature of ~ −52 °C. It may be possible that this limit is lowered with further microorganism studies, in which case our Martian simulations demonstrate that S_l and d_r will continue to support habitability under these colder conditions. However, it is important to remember that as temperatures approach the eutectic of a particular salt, the concentration of that salt's constituent ions in the residual liquid will increase dramatically. Organisms persisting in this environment would have to be both psychrophilic and extremely halotolerant. Perchlorates pose heightened challenges to both single and multi-cellular organisms relative to other salts. Experiments on select eukaryotic microorganisms (some of the most perchlorate-tolerant species on Earth) have shown a decrease in salt tolerance from $NaClO_4$ to $Mg(ClO_4)_2$ to $Ca(ClO_4)_2$, which may be connected to the chaotropicity of the salts (Heinz et al., 2021; Rzymski et al., 2024). Chaotropicity characterizes the ability of a solute to disrupt the hydrogen bonding network between water molecules and reduce the stability of the native state of proteins by weakening their hydrophobic effect. Chaotropicity correlates with eutectic temperature, among other physiochemical parameters. The physiochemical characteristics that allow perchlorate salt species to produce substantial residual liquid in the ice-soil matrix at progressively lower eutectic temperatures may pose correspondingly greater challenges to cell maintenance at high concentrations. The role of individual physiochemical parameters in brine habitability is complex. Payler et al. (2019) emphasized that "total ionic composition, which is responsible for [a brine's] specific physicochemical profile [is likely] to be the barrier to microbial propagation, rather than any one individual physicochemical parameter." Thus, the complexity of halotolerance in terrestrial organisms reinforces the importance of considering multiple habitability criteria for Mars, where there is likely to be an interplay between kinetic limitations to metabolism due to temperature, as well as physiochemical limitations imposed by near-eutectic concentrations of various salt species (c.f. Chevrier et al., 2022).

Of the four habitability metrics (T, a_w, S_l, d_r) examined here, S_l and d_r may commonly be the least restrictive. Provided that modest concentrations of salts occur in the permafrost of either Mars or Antarctica, summertime S_l and d_r can exceed habitable threshold values of 5 % and 1 μm, respectively. These habitable conditions (S_l and d_r) can occur not only whenever T and a_w are within habitable limits (i.e., greater than −40 °C and 0.6), but can also extend to colder and dryer conditions, regionally and with depth, controlled in large part by the eutectic temperature and concentration of the salt species present. Therefore, the dominant limitation to shallow ground-ice habitability is the more restrictive conditions of T and a_w. Of these two habitability criteria, the spatial range and depth distribution of temperature places a tighter constraint on locations of potential habitability (Rivera-Valentín et al., 2020; Mellon et al., 2024). As discussed previously, the temperature limits are based on observations of terrestrial organisms and their ability to either propagate or undergo maintenance metabolism. While growth requires temperatures > −18 °C, maintenance metabolism has been observed at −33 °C, possibly as low as −40 °C (e.g., Bakermans and Skidmore, 2011; Sowers, 2001; Panikov et al., 2006; de Vera et al., 2014). In addition, the −40 °C "extreme metabolic limit" by itself does not appear to be a cutoff, but a point along a rapidly decreasing metabolic rate. The ready availability of residual liquid at −40 °C may extend this boundary slightly for Mars, but cannot mitigate the fundamental kinetic constraints.

5.2. Implications for Mars landing site selection

We previously provided landing site selection guidance for modern life-detection experiments on Mars, based on simulations of historical ice temperature and water activity only (Mellon et al., 2024). We assumed that science mission objectives were, broadly, to search for extant life and assess modern habitability, and that such a mission would carry a drill capable of sampling the upper ~2 m of dry and icy permafrost (e.g., Putzig et al., 2019; National Academies of Sciences, Engineering, and Medicine, 2023), with the specific goals of accessing ground ice, to examine current ice chemistry, recent climate history and habitability conditions, and to search for organic biomarkers, as well as live, dormant, or fossil organisms. We divided potential northern hemisphere landing sites into three latitude ranges, which provided opportunities to analyze ice in distinct stratigraphic zones based on the presence or absence of extant ice, the age of extant ice, and ice temperature history. We have expanded this landing site classification scheme to reflect the range of latitudes and depths where S_l and d_r have periodically reached habitable values in a Phoenix-like soil containing 1 wt% $Mg(ClO_4)_2$.

There are three critical divisions in our original classification (Fig. 9a). First, the *current* presence or absence of *thermally stable* ice in the upper 1–2 m defines a sharp latitudinal divide between locations where we can confidently expect to sample ice (~47° N and poleward) and locations equatorward of ~47° N where there is a substantial risk of only having access to desiccated regolith in the upper meter. A second latitudinal divide occurs at 59°N. Equatorward of this divide, the upper ~2 m of regolith has experienced periodic episodes of complete desiccation between periods of ice saturation. Poleward of 59° N, ground ice has been continuously present in the upper meter for millions of years. The third critical division in Fig. 9a is stratigraphic; in the uppermost decimeters of the regolith, temperatures have periodically exceeded the −40 °C extreme metabolic limit; we deemed deeper ice "never habitable," remaining below −40 °C at all times. Water activity in this region periodically exceeded the threshold of 0.6, but we considered

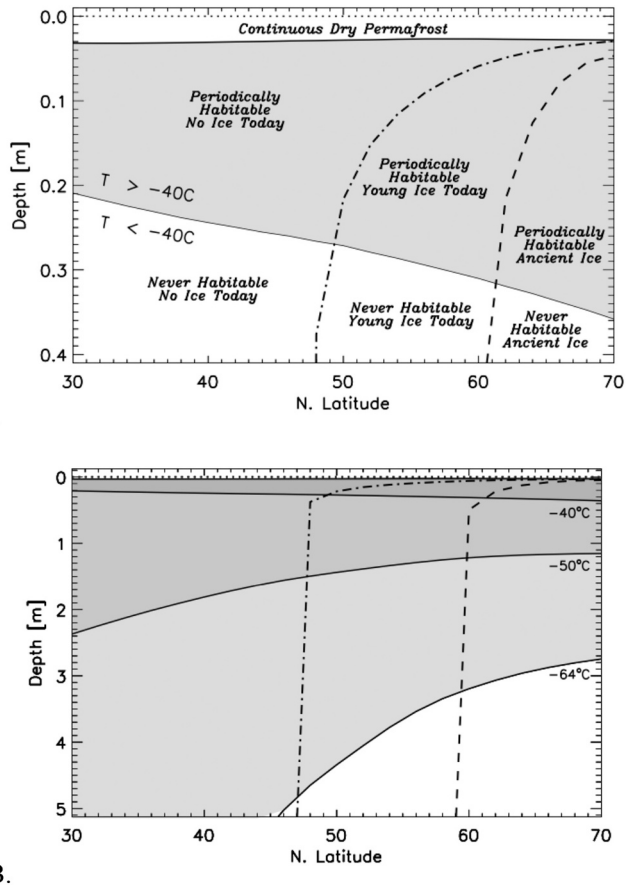


Fig. 9. Schematics of ice accessible to lander-based bore-hole habitability experiments: (a) from Mellon et al., 2024, (b) expanded to consider $S_l > 5$ % and $d_r > 1$ μm habitability criteria. In (a) the grey shaded region indicates locations where ground ice can achieve habitable values of $T > -40$ °C when ice is present. In (b) grey shades indicate regions where S_l and d_r may achieve habitable values. Habitable ice (grey region in a; darkest grey region in b) can occur only at shallow depths (<0.5 m) where ice temperatures have periodically exceeded the extreme metabolic limit of −40 °C and all four parameters (T, a_w, S_l, d_r) have simultaneously met habitability criteria during high obliquity excursions. In regions where temperatures never exceed the $Mg(ClO_4)_2$ eutectic of ~ − 64 °C none of these four parameters ever reach habitable values. In regions where peak temperatures are intermediate between the extreme metabolic limit and the $Mg(ClO_4)_2$ eutectic, whether or not S_l and d_r have periodically exceeded habitable values is primarily dependent upon the concentration of $Mg(ClO_4)_2$. For 1 dry wt% $Mg(ClO_4)_2$ and higher concentrations, habitable values of S_l and d_r can extend to the depths indicated by the solid line at −64 °C. For lower concentrations of $Mg(ClO_4)_2$, habitable values of S_l and d_r will be restricted to higher temperatures and shallower depths, as approximately represented by the solid line at −50 °C. Note that we can confidently expect to excavate ice poleward of ~47–49° N and the latitude range in which ancient ice in the top meters of regolith has been protected from periodic desiccation occurs poleward of 59° N.

temperature the dominant habitability restriction, a choice consistent with previous studies (e.g., Rivera-Valentín et al., 2020).

In our new analysis of S_l and d_r in a Phoenix-like soil with 1 wt% magnesium perchlorate, habitable values of S_l and d_r extend from the ice table down through the −40 °C horizon to the eutectic temperature (−64 °C) (see Figs. 3 and 4). This unfrozen-water condition defines a deeper stratigraphic horizon that may be important for life-detection missions as well as the evolution of ice chemistry (Fig. 9b). Above this depth, significantly mobile unfrozen water may be available and below this depth none of the four habitability criteria (T, a_w, S_l, d_r) have been met during the past few million years. Of these conditions, the extreme metabolic limit of −40 °C still represents the most restrictive condition and shallowest horizon (Mellon et al., 2024). However, this limit is set by current observations of metabolism in terrestrial microorganisms (e.g., de Vera et al., 2014; Rummel et al., 2014) and it may potentially extend below −40 °C (Price and Sowers, 2004).

Between the −40 °C and − 64 °C horizons, up to three habitability criteria (a_w, S_l, d_r) may be periodically met, dependent up on the specific concentrations of available perchlorate and other low-eutectic temperature salts. However, temperatures remaining below the extreme metabolic limit of −40 °C prevent this depth horizon from being considered potentially habitable. Fulfilling all four habitability parameters simultaneously (T, a_w, S_l, d_r) would be necessary to establish habitable conditions.

There are two extended longitudinal regions in the northern hemisphere where ice has been detected equatorward of the thermal stability boundary (~47° N), via visible exposures in craters and on scarps (e.g., Dundas et al., 2014; Dundas et al., 2021; Dundas et al., 2022), via neutron spectroscopy (e.g., Pathare et al., 2018), and via thermal techniques (Putzig et al., 2023). This ice is commonly hypothesized to be a relict of past climate conditions, e.g. buried snow or glacial ice, and there is considerable uncertainty in its burial depth, lateral continuity, and volumetric structure (Putzig et al., 2023). This ice may have exhibited significant levels of residual liquid in the past if substantial dust and low-eutectic salts are intermixed with the ice. However, uncertainty in the burial depth and volumetric concentration of this ice (i.e. the question of whether it is pore filling or massive) prevents us from modeling past residual liquid in these regions. Further, current ice-table depths in these regions are approximated to be decimeters to >1 m, indicating the existing ice there is too deep to have experienced habitable temperatures in recent history. Substantial lateral heterogeneity in ice-table depths of low-latitude relict ice also pose a risk of failure to sample icy material for landed spacecraft.

Thus, our current recommendations for landing site selection are broadly unchanged from our previous paper (Mellon et al., 2024), but the new results offer some more nuanced insights. We reiterate that high-latitude sites (>59° N) are most desirable, because they offer multiple key elements toward achieving mission goals and objectives. Specifically, sites poleward of 59°N assure access to ice and offer a maximum number of stratigraphic ice layers with distinct ages and habitability histories, potentially allowing comparisons between geologically young ice (100 s of kyr) and ancient ice (> > 1 Myr), with some ice in each age category having periodically experienced habitable values of the four parameters we considered. Most critically, this latitude zone offers access to permafrost that has not experienced 1–2 m deep desiccation as recently as the past few hundred thousand years, optimizing preservation of organisms and/or biosignatures.

We also note that high latitude landing sites (>59° N) may be advantageous in terms of investigating transport of residual liquid, solutes, and nutrients. Observations of local stratigraphic concentrations of solutes and/or ice lenses, if present, could provide valuable insights into the long-term mobility of residual water below the ice table, and the range of depths over which habitability should be assessed. *Re*-visiting the Phoenix landing site (or another location at the same latitude), where localized excess ice was observed in close proximity to pore-filling ice, would be particularly advantageous. At latitudes poleward of 61°N ancient ice (Myr) exists at depths shallow enough to reach −40 °C. An assessment of whether excess ice observed in the Goldilocks trench at the Phoenix site is an ice lens (Mellon et al., 2009), and a search for similar structures in the subsurface, could provide direct validation of models of residual liquid fraction and liquid mobility in the icy permafrost (Sizemore et al., 2015). Determining the vertical distribution of localized excess ice would also indicate whether pure ice bodies impose a substantial barrier to diffusion of nutrients through liquid vein networks in the very shallow regolith (Ostroumov and Siegert, 1996).

Landing sites in the middle latitudes (49°-59° N) offer fewer stratigraphic layers, and preclude access to ancient habitable ice, but still assure access to present-day ground ice, as well as ice horizons that both

have and have not experienced all the habitable conditions (T, a_w, S_l, d_r) within the upper meter, and dry permafrost that was previously ice-rich and habitable in the past Myrs. Candidate ice lenses or segregation ice like that observed at the Phoenix landing site might also be detectible. However, accessible materials in the upper meter of this latitude zone will have been subjected to many cycles of desiccation as recently as the past few hundred thousand years.

Mellon et al. (2024) deemed low-latitude sites (equatorward of 49° N) undesirable. Current, *thermally stable* ground ice-between 47° N and 49° N is several decimeters to meters beneath the surface and is too deep to have experienced habitable temperatures. The same is broadly true of *thermally unstable* ice at lower latitudes, including ice detected via radar sounding in the lowest-latitude regions of Arcadia and Utopia Planitiae (e.g., Bramson et al., 2015; Stuurman et al., 2016) and the most equatorward surface ice exposures in the northern hemisphere (e.g., Dundas et al., 2021; Dundas et al., 2022). Equatorward of 47° N stable ground ice is not expected to occur in the upper 2 m. The currently ice-free regolith (dry permafrost) in this region is expected to have been ice-rich during higher obliquity. This past ice would have experienced habitable ranges of all four conditions (T, a_w, S_l, d_r). Today, potential biomarkers from that time may be present, but shallow *accessible* ice <1 m deep, which also serves to preserve such biomarkers, cannot be confidently expected.

We previously (Mellon et al., 2024) cautioned against targeting a landed mission toward buried excess ice (such as a relict snow deposit) in the low latitude region, arguing that: (1) relic ice may be too deep to be accessible due to rapid sublimation; (2) the formation mechanism, modification history, and resultant subsurface structure are poorly understood; (3) the habitability history of low-latitude relic excess ice may be much more complex than in continuous icy permafrost. In addition to broadly supporting higher latitude landing sites, our current results also caution against targeting a Martian life detection mission to low-latitude massive ice deposits outside the current range of thermal ice stability, because we expect massive ice to contain minimal residual liquid and there is not a well-constrained pathway to modeling the residual liquid fraction.

The predictive techniques we have used to model residual liquid in ice-cemented soil rely on the fact that the soil pore structure effectively pins thin films and veins in place, dictating their geometry for a given liquid fraction, S_l. Uncertainties in our prediction of S_l in a frozen soil arise primarily from uncertainties in the availability of specific solutes, and secondarily from details of the grain and pore size distribution. In massive ice, without this pore structure, liquid veins occur at ice grain boundaries that are modified over time through a process called grain-ripening (e.g. Lei et al., 2022), which is dependent upon the temperature and pressure history of the ice, as well as entrained impurities. While limited modeling of vein networks in terrestrial ice cores is possible (e.g., Price, 2000; Rempel et al., 2001a, 2001b; Ng, 2021), constraining the characteristics of liquid veins in a Martian relic ice deposit of unknown age, depositional mode, temperature and burial history poses significantly more challenges. Further, laboratory studies of perchlorates indicate that intimate mixtures of soil and brine enhance the effectiveness of supercooling in ice-brine-mineral systems absent a significant gas component (Toner et al., 2014a; Shumway et al., 2023) – although experiments more representative of the vadose zone indicate that soil particles do not strongly affect the phase transitions of magnesium perchlorate exposed to controlled humidity atmospheres (Primm et al., 2018). Enhanced supercooling due to intimate mixing of ice and regolith might provide advantages for low temperature nutrient transport beyond what is reflected in our models system beneath the ice table. Finally, excess or massive ice is generally less pervious than adjacent ice-saturated particulate material at equivalent temperature (Ostroumov and Siegert, 1996; Rempel, 2007, 2008; Sizemore et al., 2015).

We previously deemed relic ice a "risky and unpredictable target" in terms of its burial depth and modification history. Our new results emphasize that relic ice is a risky and unpredictable target in terms of its residual liquid content and ability to facilitate nutrient/waste transport for organisms. Targeting a landing site poleward of 47°N where we have substantial predictive ability provides the best opportunities to test the boundaries of our current understanding and to extrapolate local observations of residual water to global trends.

6. Conclusions

We have developed new soil freezing curves (SFCs) describing the residual liquid content and liquid-vein geometry for examples of "Martian" and "Antarctic" soils below the bulk freezing temperature of 0 °C. We used empirical particle size distributions measured for Beacon Valley soil samples (Sizemore and Mellon, 2008) and regolith at the Phoenix landing site (Pike et al., 2011) to build synthetic soil packings for "Antarctic" and "Martian" soils, respectively, and derived SFCs via Monte Carlo simulations of soil freezing (Chen et al., 2020). We considered the effects of salt doping on both soil geometries, using examples of: (1) magnesium perchlorate, $Mg(ClO_4)_2$, as an example low-eutectic-temperature solute representative of Martian solutes and (2) sodium chloride, NaCl, as a high-eutectic-temperature salt approximately representative of solutes in the Dry Valleys of Antarctica. We applied our SFCs to directly calculate the total liquid fraction, S_l, and maximum liquid vein diameter or refugia diameter, d_r, under relevant Martian and Antarctic environmental conditions, building on our recent survey of Martian permafrost temperature history (Mellon et al., 2024) and the field measurements of Marinova et al. (2022).

We established new habitability thresholds based on these parameters, defining habitable conditions as: (1) $S_l > 5$ %, such that a liquid vein network is connected enough to allow transport of nutrients and wastes to organisms; and (2) $d_r > 1$ μm, such that approximately micron-scale cellular organisms can be fully immersed and possibly mobile inside liquid veins. These habitability metrics exist in concert with previous metrics of temperature and water activity (T and a_w) with habitable thresholds of > -40 °C and > 0.6, respectively (see Rummel et al., 2014; Mellon et al., 2024). In this context, we carried out self-consistent simulations of T, a_w, S_l, and d_r and we examined which of these four metrics presents the dominant restriction to shallow-ice habitability in the Martian environment and in University Valley, Antarctica. We also revisited discussion of optimal landing site selection for Mars life and habitability exploration missions. We have found that:

Environmentally available solutes are likely to be the dominant factor controlling low-temperature liquid availability in the icy permafrost of Mars and in the highest altitude Antarctic Dry Valleys where ground ice does not experience excursions above the bulk melting temperature 0 °C.

Soil geometry (particle and pore-size distributions) play a secondary but still important role in determining whether S_l and d_r meet habitability thresholds under a given set of environmental conditions. The synthetic soil packings we built are applicable to both the Antarctic and Martian environments, despite their basis in in situ data from different planetary settings.

Without salts, neither of the examined soil geometries produce habitable values of S_l or d_r below ~ -3 °C based on pore-confinement effects alone. The addition of 1 dry wt% NaCl extends the occurrence of habitable values of S_l and d_r to the eutectic temperature of −21 °C; the addition of 1 dry wt% $Mg(ClO_4)_2$ extends the occurrence of habitable values of S_l and d_r to the magnesium perchlorate eutectic temperature of −64 °C, well below the previously defined extreme metabolic limit of $T = -40$ °C. This finding leads us to conclude that meeting the requirement of $d_r > 1$ μm and $S_l > 5$ % is surprisingly easy for silty to sandy soils with plausible salt doping in the Martian and Antarctic environments.

In the University Valley environment, localized solute deficits may preclude habitable S_l and d_r even in the "warm" austral summer when conventional T and a_w thresholds for metabolism are met. However, we generally expect available chlorides and nitrates to produce habitable values of T, a_w, S_l, and d_r simultaneously in the summer months in

University Valley. On Mars, local deficits in perchlorate and nitrate concentrations may prevent S_l and d_r from reaching habitable values even under idealized summertime, high obliquity conditions, but in general, we expect abundant perchlorates in the unconsolidated regolith to produce habitable values of S_l and d_r below T and a_w habitability thresholds. Thus, there is an Antarctic scenario in which S_l is the most restrictive habitability criterion (i.e., lack of residual water precludes habitability at warm temperatures), and a Martian scenario in which T, but not S_l or d_r, is the most restrictive criterion (i.e., extreme cold precludes habitability despite the existence of a well-connected liquid vein network).

For a Phoenix-like soil containing 1 dry wt% magnesium perchlorate on Mars, high-obliquity "relatively-clement" periods can produce summertime $S_l > 5$ % and $d_r > 1$ μm for periods of 10s of kyrs repeatedly over the past 2.5 Ma for all latitudes poleward of 30°N (e.g., Fig. 7). These periods of habitable conditions last longer and both parameters achieve higher values at higher latitudes. Furthermore, our simulations show that for Phoenix-like soils poleward of 50°N, 1 wt% $Mg(ClO_4)_2$ produces $S_l \sim 6$ % and $d_r > 5$ μm *in the current climate*, whereas ground ice itself is predicted to be currently stable poleward of ~47°N (Mellon et al., 2024). However, the coarser-grained Beacon soil with magnesium perchlorate doping does not meet habitability thresholds for both parameters in the current Martian climate, indicating that the independent effects of grain-size distribution on pore confinement and thermal inertia can locally or regionally tip the balance for liquid availability and habitability. In our simulations of Martian permafrost with magnesium perchlorate, S_l and d_r were never the dominant limitations to habitability. This result raises the possibility that temperature thresholds for life based on terrestrial organisms in terrestrial environments should be considered more holistically for Mars.

In University Valley, Antarctica, a deficit of perchlorates relative to Mars likely restricts habitable S_l and d_r to the summer months, when temperatures are above the eutectic of NaCl and other chlorides. Observed vertical and regional variation in the concentrations of soluble ion species raises the possibility that ice in some parts of University Valley never reaches habitability thresholds despite warm temperatures due to local, extremely low concentrations of a wide range of salt species. Thus, solute availability may be the dominant habitability restriction in "warm" Antarctic Dry Valley conditions. New surveys of soluble ion concentrations in University and Beacon Valleys, as well as targeted development of SFCs for specific Dry Valley weather-station and borehole locations could substantially expand our understanding of temporal and spatial variability of conditions supporting metabolism.

Our simulations provide landing site selection guidance for a Mars life-detection mission broadly similar to our previous survey of Martian ground ice temperature history (Mellon et al., 2024). We recommend landing sites poleward of 49°N, which provide confidence in access to ice that has periodically experienced "habitable" conditions as defined by all four parameters (T, a_w, S_l, and d_r). Equatorward of 47° - 49° N, there is risk of failing to encounter ice. Poleward of 49° N, higher-latitude landing sites offer progressively greater opportunities to compare ice across stratigraphic layers defined by distinct ages and habitability histories. Between ~47° and 50° N ice is too deep to have met the extreme metabolic limit of $T = -40$ °C in the past few Myr; additionally, d_r and S_l do not reach "habitable" values during current summertime conditions. Between 50° and 59° N ice has periodically met all four habitability thresholds, but the soil column has also been periodically desiccated to depths of 1–2 m in the last several hundred thousand years. Poleward of 59° ice has been continuously present in the upper 1–2 m and younger, shallower ice has been periodically habitable. Poleward of 61° ice has been continuously present for Myr and some of this ancient ice has also met all four habitability criteria (T, a_w, S_l, and d_r). Everywhere poleward of 50° N 1 wt% $Mg(ClO_4)_2$ can produce $S_l > 5$ % and $d_r > 1$ μm in a Phoenix-like soil under current summer-time conditions. Landing sites poleward of 61° N offer the best opportunities to sample and compare ice of different ages and distinct habitability histories.

Our results also indicate that massive ice is a less desirable target than pore-filling ice at all latitudes. Absent confinement effects of the soil pore space, clean low-temperature ice will have a lower liquid fraction, lower permeability, and lower effective diffusion coefficients for ion transport than adjacent soil-ice mixtures, restricting S_l and d_r, and thus habitability.

CRediT authorship contribution statement

H.G. Sizemore: Writing – original draft, Software, Project administration, Methodology, Investigation, Funding acquisition, Formal analysis, Data curation, Conceptualization. **M.T. Mellon:** Writing – review & editing, Software, Methodology, Formal analysis, Conceptualization. **A. W. Rempel:** Writing – review & editing, Software, Methodology, Investigation, Funding acquisition, Formal analysis. **C.P. McKay:** Writing – review & editing, Methodology, Data curation, Conceptualization. **J.L. Heldmann:** Writing – review & editing, Methodology, Investigation, Conceptualization. **C.R. Stoker:** Writing – review & editing, Methodology, Conceptualization. **M.R. Perry:** Writing – review & editing, Validation, Software.

Funding information

This work was partially supported by the NASA Solar System Workings program via grant 80NSSC18K0012.

Declaration of competing interest

The authors declare that they have no known competing financial interests or personal relationships that could have appeared to influence the work reported in this paper.

Acknowledgements

We would like to thank Dr. Rachel A. Slank (Lunar and Planetary Institute) and Vera Demchenko (Lockheed Martin) for early conversations related to this study. This work was partially supported by the NASA Solar System Workings program via grant 80NSSC18K0012.

Data availability

Data will be made available on request.

References

Andersland, O.B., Ladanyi, B., 2004. An Introduction to Frozen Ground Engineering. CRC Press, Boca Raton, FL, p. 363.

Archer, P.D., Franz, H.B., Sutter, B., Arevalo Jr., R.D., Coll, P., Eigenbrode, J.L., McAdam, A.C., McKay, C.P., Ming, D.W., Morris, R.V., Navaro-Gonzáles, R., Niles, P. B., Pavlov, A., Squyres, S.W., Stern, J.C., Steele, A., Wray, J.J., 2013. Abundances and implications of volatile-bearing species from evolved gas analysis of the Rocknest aeolian deposit, Gale crater. Mars. J. Geophys. Res. Planets 119, 237–254. https://doi.org/10.1002/2013JE004493.

Archer, P.D., Sutter, B., McAdam, A.C., Stern, J.C., Clark, J.V., Lewis, J.M., Franz, H.B., Pavlov, A.A., Eigenbrode, J.L., Knudsen, C.A., 2024. Oxychlorines and nitrates in Gale crater: a puzzle. In: 10th international conference on Mars, No. 3007.

Bakermans, C., 2008. Limits for microbial life at subzero temperatures. In: Psychrophiles: from Biodiversity to Biotechnology. Springer Berlin Heidelberg, Berlin, Heidelberg, pp. 17–28.

Bakermans, C., Skidmore, M., 2011. Microbial respiration in ice at subzero temperatures (− 4 C to− 33 C). Environ. Microbiol. Rep. 3 (6), 774–782.

Bass, G.W., 1980. Stability of brines on Mars. Icarus 42, 20–28. https://doi.org/10.1016/0019-1035(80)90237-7.

Beaty, D., Clifford, S.M., Borg, L.E., Catling, D.C., Craddock, R.A., Des Marais, J., Farmer, J.D., Frey, H.G., Haberle, R.M., McKay, C.P., Newsom, H.E., Parker, T.J., Segura, R., Tanaka, K.L., 2005. Key science questions from the second conference on early Mars: geologic, hydrologic, and climatic evolution and the implications for life. Astrobiology 5. https://doi.org/10.1089/ast.2005.5.663.

Bramson, A.M., Byrne, S., Putzig, N.E., Sutton, S., Plaut, J.J., Brothers, T.C., 2015. Widespread excess ice in Arcadia Planitia. Mars. Geophys. Res. Let. 42 (16), 6566–6574. https://doi.org/10.1002/2015GL064844.

Carrier, B.L., Kounaves, S.P., 2015. The origins of perchlorate in the Martian soil. Geophys. Res. Lett. 42, 3739–2745.
Catling, D.C., Claire, M.W., Zahnle, K.J., Quinn, R.C., Clark, B.C., Hecht, M.H., Kounaves, S., 2010. Atmospheric origins of perchlorate on Mars and in the Atacama. J. Geophys. Res. Planets 115. https://doi.org/10.1029/2009JE003425.
Chen, J., Mei, S., Irizarry, J.T., Rempel, A.W., 2020. A Monte Carlo approach to approximating the effects of pore geometry on the phase behavior of soil freezing. Journal of Advances in Modeling Earth Systems 12, e2020MS002117. https://doi.org/10.1029/2020MS002117.
Chevrier, V.F., Hanley, J., Altheide, T.S., 2009. Stability of perchlorate hydrates and their liquid solution at the Phoenix landing site. Mars. Geophys. Res. Let. 36. https://doi.org/10.1029/2009GL037497.
Chevrier, V.F., Fitting, A.B., Rivera-Valentín, E.G., 2022. Limited stability of multicomponent brines on the surface of Mars. Planet. Sci. J. 3 (125). https://doi.org/10.2847/PSJ/ac6603.
Clarke, A., Morris, G.J., Fonseca, F., Murray, B.J., Acton, E., Price, H.C., 2013. A low temperature limit for life on earth. PLoS One 8 (6), e66207.
Dash, J.G., Rempel, A.W., Wettlaufer, J.S., 2006. The physics of premelted ice and its geophysical consequences. Rev. Mod. Phys. 78, 695–741. https://doi.org/10.1103/RevModPhys.78.695.
de Vera, J.P., Schulze-Makuch, D., Khan, A., Lorek, A., Koncz, A., Möhlmann, D., Spohn, T., 2014. Adaptation of an Antarctic lichen to Martian niche conditions can occur within 34 days. Planet. Space Sci. 98, 182–190.
Dundas, C.M., Byrne, S., McEwen, A.S., Mellon, M.T., Kennedy, M.R., Daubar, I.J., Saper, L., 2014. HiRISE observations of new impact craters exposing Martian ground ice. J. Geophys. Res. Planets 119, 109–127. https://doi.org/10.1002/2013JE004482.
Dundas, C.M., Mellon, M.T., Conway, S.J., Daubar, I.J., Williams, K.E., Ojha, L., Wray, J. J., Bramson, A.M., Byrne, S., McEwen, A.S., Posiolova, L.V., Speth, G., Viola, D., Landis, M.E., Morgan, G.A., Pathare, A.V., 2021. Widespread Exposures of Extensive Clean Shallow Ice in the Midlatitudes of Mars. J. Geophys. Res, Planets 126. https://doi.org/10.1029/2020JE006617.
Dundas, C.M., Mellon, M.T., Posiolova, L.V., Milijkovic, K., Collins, G.S., Tornabene, L.L., Rangarajan, V.G., Golombeck, M.P., Warner, N.H., Daubar, I.J., Byrne, S., McEwen, A.S., Seelos, K.D., Viola, D., Bramson, A.M., Speth, G., 2022. A large new crater exposes the limits of water ice on Mars. Geophys. Res. Lett. 50. https://doi.org/10.1029/2022GL100747.
Farley, K.A., 117 co-authors, 2022. Aqueously altered igneous rocks sampled on the floor of Jezero crater. Mar. Sci. 377, 1512. https://doi.org/10.1126/science.abo2196.
Fischer, E., Martínez, G.M., Rennó, 2016. Formation and persistence of brine on Mars: experimental simulations throughout the diurnal cycle at the Phoenix landing site. Astrobiology 16. https://doi.org/10.1089/ast.2016.1525.
Fischer, E., Martínez, G.M., Elliott, H.M., Rennó, 2014. Experimental evidence fro the formation of liquid saline water on Mars. Geophys. Res. Lett. 41, 4456–4462. https://doi.org/10.1002/2014GL060302.
Fox-Powell, M.G., Hallsworth, J.E., Cousins, C.R., Cockell, C.S., 2016. Ionic strength is a barrier to the habitability of Mars. Astrobiology 16 (6). https://doi.org/10.1089/ast.2015.1432.
Fukazawa, H., Sugiyama, K., Mae, S.J., Narita, H., Hondoh, T., 1998. Acid ions at triple junction of Antarctic ice observed by Raman scattering. Geophys. Res. Lett. 25, 2845–2848. https://doi.org/10.1029/98GL02178.
Gough, R.V., Chevier, V.F., Baustian, K.J., Wise, M.E., Tobert, M.A., 2011. Laboratory studies of perchlorate phase transitions: Support for metastable aqueous perchlorate solutions on Mars. Earth and Planetary Science Letters 312, 371–377. https://doi.org/10.1016/j.epsl.2011.10.026.
Gough, R.V., Chevrier, V.F., Tolbert, M.A., 2016. Formation of liquid water at low temperatures via the deliquescence of calcium chloride: implications for Antarctica and Mars. Planet. Space Sci. 131, 79–87. https://doi.org/10.1016/j.pss.2016.07.006.
Gough, R.V., Nuding, D.L., Martínez, G.M., Rivera-Valentín, E.G., Primm, K.M., Tolbert, M.A., 2023. Laboratory studies of brine growth kinetics relevant to deliquescence on Mars. The Planetary Science Journal 4, 46. https://doi.org/10.3847/PSJ/acbd98.
Hall, D.L., Sterner, S.M., Bodnar, R.J., 1988. Freezing Point Depression of NaCl-KCl-H_2O Solutions. Economic Geology 83, 197–202. https://doi.org/10.2113/gsecongeo.83.1.197.
Hardy, S.C., 1977. A grain boundary groove measurement of the surface tension between ice and water. Philos. Mag. 35 (2), 471–484. https://doi.org/10.1080/14786377708237066.
Hecht, M.H., Kounaves, S.P., Quinn, R.C., Young, S.M.M., Ming, D.W., Catling, D.C., Clark, B.C., Boynton, W.V., Hoffman, J., DeFlores, L.P., Gospodinova, K., Kapit, J., Smith, P.H., 2009. Detection of perchlorate and the soluble chemistry of martian soil at the Phoenix lander site. Science 325, 64–67. https://doi.org/10.1126/science.1172466.
Heinz, J., Rambags, V., Schulze-Makuch, D., 2021. Physiochemical parameters limiting growth of Debaryomyces hansenii in solutios of hygroscopic compounds and their effects on the habitability of martian brins. Life (Basel) 11, 1194.
Heldmann, J.L., Marinova, M.M., Lim, D.S., Wilson, D., Carrato, P., Kennedy, K., Esbeck, A., Colaprete, A., Elphic, R.C., Captain, J., Zacny, K., 2022. Mission architecture using the SpaceX starship vehicle to enable a sustained human presence on Mars. New Space 10 (3), 259–273.
Israelachvili, J.N., 2011. Intermolecular and Surface Forces – 3rd Ed. Academic press as an imprint of Elsevier. ISBN: 978-0-12-391927-4.
Jakosky, B.M., Henderson, B.G., Mellon, M.T., 1993. The Mars water cycle at other epochs: recent history of the polar caps and layered terrain. Icarus 102, 286–297. https://doi.org/10.1006/icar.1993.1049.
Jakosky, B.M., Nealson, K.H., Bakermans, C., Ley, R.E., Mellon, M.T., 2003. Subfreezing activity of microorganisms and the potential habitability of Mars' polar regions. Astrobiology 3, 343–350. https://doi.org/10.1089/153110703769016433.
Jaramillo, E.A., Royle, S.H., Claire, M.W., Kounaves, S.P., Sephton, M.A., 2019. Indigenous organic-oxidized fluid interactions in the Tissint Mars meteorite. Geophys. Res. Lett. 46, 3090–3098. https://doi.org/10.1029/2018GL081335.
Kounaves, S.P., Hecht, M.H., Kapit, J., Gospodinova, K., DeFlores, L., Quin, R.C., Boynton, W.V., Clark, B.C., Catling, D.C., Hredzak, P., Ming, D.W., Moore, Q., Shusterman, J., Stroble, S., West, J., Young, S.M.M., 2010. Wet chemistry experiments on the 2007 Phoenix Mars scout Lander mission: data analysis and results. J. Geophys. Res. Planets 115. https://doi.org/10.1029/2009JE003424.
Kounaves, S.P., Carrier, B.L., O'Neil, G.D., Stroble, S.T., Claire, M.W., 2014. Evidence of martian perchlorate, chlorate, and nitrate in Mars meteorite EETA79001: implications for oxidants and organics. Icarus 229, 206–213. https://doi.org/10.1016/j.icarus.2013.11.012.
Laskar, J, Correia, A. C. M., Gastineau, M., Joutel, F., Levrard, B., Robutel, P., 2004. Long term evolution and chaotic diffusion of the insolation quantities of Mars. Icarus, 170, 343–364, doi: https://doi.org/10.1016/j.icarus.2004.04.005.
Lei, P., Young, M.W., Seymour, J.D., Stillman, D.E., Primm, K., Sizemore, H.G., Rempel, A.W., 2022. NMR characterization of unfrozen brine vein distribution and structure in model packed beds. Cold Reg. Sci. Technol. 199, 103572. https://doi.org/10.1016/j.coldregions.2022.103572.
Lynch, K.L., Jackson, W.A., Rey, K., Spear, J.R., Rosenzweig, F., Munakata-Marr, J., 2019. Evidence for biotic perchlorate reduction in naturally perchlorate-rich sediments of pilot Valley Basin Utah. Astrobiology 19 (5). https://doi.org/10.1089/ast.2018.1864.
Marinova, M.M., McKay, C.P., Pollard, W.H., Heldman, J.L., Davila, A.F., Andersen, D.T., Jackson, W.A., Lacelle, D., Paulsen, G., Zacny, K., 2013. Distribution of depth to ice-cemented soils in the high-elevation Quartermain Mountains, McMurdo dry valleys, Antarctica. Antarct. Sci. 25 (4), 575–582. https://doi.org/10.1017/S095410201200123X.
Marcus, Y., 2017. Unconventional Deep Eutectic Solvents: Aqueous Salt Hydrates. ACS Sustainable Chem. Eng. 5, 11780–11787. https://doi.org/10.1021/acssuschemeng.7603528.
Marinova, M.M., McKay, C.P., Heldmann, J.L., Goordial, J., Lacelle, D., Pollard, W.H., Davila, A.F., 2022. Climate and energy balance of the ground in University Valley, Antarctica. Antarct. Sci. 34 (2), 144–171. https://doi.org/10.1017/S0954102022000025.
McKay, C.P., Mellon, M.T., Friedmann, E.I., 1998. Soil temperatures and stability of ice-cemented ground in the McMurdo dry valleys, Antarctica. Antarct. Sci. 10 (1), 31–38. https://doi.org/10.1017/S0954102098000054.
Mellon, M.T., Jakosky, B.M., 1993. Geographic variations in the thermal and diffusive stability of ground ice on Mars. J. Geophys. Res. 98, 3345–3364. https://doi.org/10.1029/92JE02355.
Mellon, M.T., Phillips, R.J., 2001. Recent gullies on Mars and the source of liquid water. J. Geophys. Res. 106, 23165–23179. https://doi.org/10.1029/2000JE001424.
Mellon, M.T., Sizemore, H.G., 2022. The history of ground ice at Jezero crater Mars and other past, present, and future landing sites. Icarus 371, 114667. https://doi.org/10.1016/j.icarus.2021.114667.
Mellon, M.T., Jakosky, B.M., Kieffer, H.H., Christensen, P.R., 2000. High-resolution thermal inertia Mappy from the Mars global surveyor thermal emission spectrometer. Icarus 148, 437–455. https://doi.org/10.1006/icar.2000.6503.
Mellon, M.T., Feldman, W.C., Prettyman, T.H., 2004. Ther presence and stability of ground ice in the southern hemisphere of Mars. Icarus 169, 324–340. https://doi.org/10.1016/j.icarus.2003.10.022.
Mellon, M.T., Arvidson, R.E., Sizemore, H.G., Searls, M.L., Blaney, D.L., Cull, S., Hecht, M.H., Heet, T.L., Keller, H.U., Lemmon, M.T., Markiewicz, W.J., Ming, D.W., Morris, R.V., Pike, W.T., Zent, A.P., 2009. Ground ice at the Phoenix landing site: stability state and origin. J. Geophys. Res. 141. https://doi.org/10.1029/2009JE003417.
Mellon, M.T., Sizemore, H.G., Heldmann, J.L., McKay, C.P., Stoker, C.R., 2024. The habitability conditions of possible Mars landing sites for life exploration. Icarus 408, 115836. https://doi.org/10.1016/j.icarus.2023.115836.
Ming, D.W., 449 co-authors, 2013. Volatile and organic compositions of sedimentary rocks in Yellowknife Bay, Gale crater. Mar. Sci. 343. https://doi.org/10.1126/science1245267.
Morgan, G.A., Putzig, N.E., Perry, M.R., Sizemore, H.G., Bramson, A.M., Petersen, E.I., Bain, Z.M., Baker, D.M.H., Mastrogiuseppe, M., Hoover, R.H., Smith, I.B., Pathare, A., Dundas, C.M., Campbell, B.A., 2021. Availability of subsurface water-ice resources in the northern mid-latitude of Mars. Nature Astronomy 5, 230–236. https://doi.org/10.1038/s41550-020-01290-z.
Morillon, V., Debeaufort, F., Jose, J., Tharrault, J.F., Capelle, M., Blond, G., Voilley, A., 1999. Water vapour pressure above saturated salt solutions at low temperatures. Fluid Phase Equilibria 155, 297–309. https://doi.org/10.1016/S0378-3812(99)00009-6.
Murphy, D.M., Koop, T., 2005. Review of the vapour pressures of ice and supercooled water for atmospheric applications. Q. J. R. Meteorol. Soc. 131, 1539–1565. https://doi.org/10.1256/qj.04.94.
National Academies of Sciences, Engineering, and Medicine, 2023. Origins, Worlds, and Life: A Decadal Strategy for Planetary Science and Astrobiology 2023–2032. The National Academies Press, Washington, DC. https://doi.org/10.17226/26522.
Ng, F.S., 2021. Pervasive diffusion of climate signals recorded in ice-vein ionic impurities. Cryosphere 15 (4), 1787–1810.
Nuding, D.L., Rivera-Valentin, E.G., Davis, R.D., Gough, R.V., Chevrier, V.F., Tolbert, M. A., 2014. Deliquescence and efflorescence of calcium perchlorate: an investigation of

stable aqueous solutions relevant to Mars. Icarus 243, 420–428. https://doi.org/10.1016/j.icarus.2014.08.036.
Nikolakakos, G., Whiteway, J.A., 2015. Laboratory investigation of perchlorate deliquescence at the surface of Mars with Raman scattering lidar. Geophys. Res. Let. 42, 7899–7906. https://doi.org/10.1002/2015FL065434.
Nuding, D.L., Davis, R.D., Gough, R.V., Tolbert, M.A., 2015. The aqueous stability of a Mars salt analog: instant Mars. J. Geophys. Res. 120, 588–598. https://doi.org/10.1002/2014JE004722.
Ostroumov, V.E., Siegert, C., 1996. Exobiological aspects of mass transfer in microzones of permafrost deposits. Adv. Space Res. 18 (12), 79–86. https://doi.org/10.1016/0273-1177(96)00002-6.
Panikov, N.S., Flanagan, P.W., Oechel, W.C., Mastepanov, M.A., Christensen, T.R., 2006. Microbial activity in soils frozen to below− 39 C. Soil Biol. Biochem. 38 (4), 785–794.
Paris, E.R., Arandia-Gorostidi, N., Klempay, B., Bowman, J.S., Pontefract, A., Elbon, C.E., Glass, J.B., Ingall, E.D., Doran, P.T., Som M.S., Sanjoy, Schmidt, B.E., Dekas, A.E., 2023. Single-cell analysis in hypersaline brines predicts a water-activity limit of microbial anabolic activity. Sci. Adv. 9 (51). https://doi.org/10.1126/sciadv.adj3594.
Pathare, A.V., Feldman, W.C., Prettyman, T.H., Maurice, S., 2018. Driven by excess? Climatic implications of new global mapping of near-surface water-equivalent hydrogen on Mars. Icaurs 301, 97–116. https://doi.org/10.1016/j.icarus.2017.09.031.
Payler, S.J., Biddle, J.F., Lollar, B.S., Fox-Powell, M.G., Edwards, T., Ngwenya, B.T., Payling, S.M., Cokell, C.S., 2019. An Ionic Limit toLife in the Deep Subsurface. Frontiers in Microbiology 10. https://doi.org/10.3389/fmicb.2019.00426.
Pike, W.T., Staufer, U., Hecht, M.H., Goetz, W., Parrat, D., Sykulska-Lawrence, H., Vijendran, S., Madsen, M.B., 2011. Quantification of the dry history of the Martian soil inferred from in situ microscopy. J. Geophys. Res. 38. https://doi.org/10.1029/2011GL049896.
Piqueux, S., Buz, J., Edwards, C.S., Bandfield, J.L., Kleinböhl, A., Kass, D.M., Hayne, P.O., the MCS & THEMIS Teams, 2019. Widespread shallow water ice on Mars at high latitudes and Midlatitudes. Geophys. Res. Lett. 46, 14290–14298. https://doi.org/10.1029/2019GL083947.
Price, P.B., 2000. A habitat for psychrophiles in deep Antarctic ice. Proc. Natl. Acad. Sci. 97, 1247–1251. https://doi.org/10.1073/pnas.97.3.1247.
Price, P.B., Sowers, T., 2004. Temperature dependence of metabolic rates for microbial growth, maintenance, and survival. Proc. Natl. Acad. Sci. 101 (13), 4631–4636.
Primm, K.M., Gough, R.V., Wong, J., Rivera-Valentín, E.G., Martinez, G.M., Hogancamp, J.V., Archer, P.D., Ming, D.W., Tobert, M.A., 2018. The effect of Mars-relevant soil analogs on the water uptake of magnesium perchlorate and implications for the near-surface of Mars. J. Geophys. Res., Planets 123 (8), 2076–2088. https://doi.org/10.1029/2018JE005540.
Putzig, N.E., Diniega, S., Dunduas, C.M., Titus, T.N., 2019. Report from the ICE and Climate Analysis Group (ICE-SAG). USGS Publications Warehouse, Astrogeology Science Center. Index ID 70204228.
Putzig, N.E., Morgan, G.A., Sizemore, H.G., Hollibaugh Baker, D.M., Petersen, E.I., Pathare, A.V., Dundas, C.M., Bramson, A.M., Courville, S.W., Perry, M.R., Nerozzi, S., Bain, Z.M., Hoover, R.H., Campbell, B.A., Mastroguiuseppe, M., Mellon, M.T., Seu, R., Smith, I.B., 2023. Ice resource mapping on Mars. In: Badescu, V., Zacny, K., Bar-Cohen, Y. (Eds.), Handbook of Space Resources, Cham. https://doi.org/10.1007/978-3-030-97913-3_16.
Qu, S.-Y., Zhao, Y.-Y.S., Cui, H., Yin, X.-Z., Jackson, W.A., Nie, X., Wu, Z.-C., Wang, J.-H., Zhou, D.-S., Qui, C., Li, X.-Y., Lui, J.-Z., 2022. Preferential formation of chlorate over perchlorate on Mars controlled by ion minerology. Nat. Astron. 6, 436–441.
Rempel, A.W., 2007. Formation of ice lenses and frost heave. J. Geophys. Res. 112, F02S21. https://doi.org/10.1029/2006JF000525.
Rempel, A.W., 2008. A theory for ice–till interactions and sediment entrainment beneath glaciers. J. Geophys. Res. 113, F01013. https://doi.org/10.1029/2007JF000870.
Rempel, A.W., 2012. Hydro-mechanical processes in freezing soils. Vadose Zone J. 11. https://doi.org/10.2136/vzj2012.0045.
Rempel, A.W., Waddington, E.D., Wettlaufer, J.S., Worster, M.G., 2001a. Possible displacement of the climate signal in ancient ice by premelting and anomalous diffusion. Nature 411, 568–571. https://doi.org/10.1038/35079043.
Rempel, A.W., Wettlaufer, J.S., Worster, M.G., 2001b. Interfacial premelting and the thermomolecular force: thermodynamic buoyancy. Phys. Rev. Lett. 87, 088501. https://doi.org/10.1103/PhysRevLett.87.088501.
Rempel, A.W., Wettlaufer, J.S., Worster, M.G., 2004. Premelting dynamics in a continuum model of frost heave. J. Fluid Mech. 498, 227–244. https://doi.org/10.1017/S0022112003006761.
Rivera-Valentín, E.G., Gough, R.V., Chevrier, V.F., Primm, K.M., Martínez, G.M., Tobert, M., 2018. Constraining the potential liquid water environment at Gale crater, Mars. J. Geophys. Res., Planets 123 (5), 1156–1167. https://doi.org/10.1002/2018JE005558.
Rivera-Valentín, E.G., Chevrier, V.F., Soto, A., Martínez, G., 2020. Distribution and habitability of (meta)stable brines on present day Mars. Nature Astronomy 4, 756–761. https://doi.org/10.1038/s41550-020-1080-9.
Rivkina, E.M., Friedmann, E.I., McKay, C.P., Gilichinsky, D.A., 2000. Metabolic activity of permafrost Bacteria below the freezing point. Appl. Environ. Microbiol. 66, 3230–3233. https://doi.org/10.1128/AEM.66.8.3233.2000.
Rummel, J.D., Beaty, D.W., Jones, M.A., Bakermans, C., Barlow, N.G., Boston, P., et al., 2014. A new analysis of Mars 'special regions', findings of the second MEPAG special regions science analysis group (SR-SAG2). Astrobiology 14, 887–968. https://doi.org/10.1089/ast.2014.1227.
Rzymski, P., Losiak, A., Heinz, J., Szukalska, M., Florek, E., Poniedziałek, B., Kaczmarek, Ł., Schulze-Makuch, D., 2024. Perchlorates on Mars: occurrence and implications for putative life on the red planet. Icarus 421, 116246. https://doi.org/10.1016/j.icarus.2024.116246.
Scheller, E.L., 65 co-authors, 2022. Aqueous alteration processes in Jezero crater, Mars – implications for organic geochemistry. Science 378, 1105–1111. https://doi.org/10.1126/science.abo5204.
Schorghofer, N., Forget, F., 2012. History and anatomy of subsurface ice on Mars. Icarus 220, 1112–1120. https://doi.org/10.1016/j.icarus.2012.07.003.
Shumway, A.O., Catlin, D.C., Toner, J.D., 2023. Regolith inhibits salt and ice crystallization in $Mg(ClO_4)_2$ brine, implying more persistent and potentially habitable brines on Mars. The Planetary Science Journal 4, 143. https://doi.org/10.3847/PSJ/ace891.
Sizemore, H.G., Mellon, M.T., 2008. Laboratory characterization of the structural properties controlling dynamical gas transport in Mars-analog soils. Icarus 197, 606–620. https://doi.org/10.1016/j.icarus.2008.05.013.
Sizemore, H.G., Zent, A.P., Rempel, A.L., 2015. Initiation and growth of martian ice lenses. Icarus 251, 191–210. https://doi.org/10.1016/j.icarus.2014.04.013.
Sowers, T., 2001. N2O record spanning the penultimate deglaciation from the Vostok ice core. J. Geophys. Res. Atmos. 106 (D23), 31903–31914.
Steele, A., Benning, L.G., Wirth, R., Siljeström, S., Fries, M.D., Hauri, E., Conrad, P.G., Rogers, K., Eigenbrode, J., Schrieber, A., Needham, A., Wang, J.H., MCubbin, F.M., Kilcoyne, D., Rodriguez Blanco, J.D., 2018. Organic synthesis on Mars by electrochemical reduction of CO2. Sci. Adv. 4. https://doi.org/10.1126/sciadv.aat5118.
Stern, J.C., Sutter, B., Jackson, W.A., Navarro-González, R., McKay, C.P., Ming, D.W., Archer, P.D., Mahaffy, P.R., 2017. The nitrate/(per)chlorate relationship on Mars. Geophys. Res. Lett. 44. https://doi.org/10.1002/2016GL072199.
Stillman, D.E., Grimm, R.E., 2011. Dielectric signatures of adsorbed and salty liquid water at the Phoenix landing site. Mars. J. Geophys. Res. 116. https://doi.org/10.1029/2011JE003838.
Stillman, D.E., Primm, K.P., Codd, S.L., Seymour, J.D., Lei, P., Sizemore, H.G., Rempel, A.W., 2019. Magnetic resonance and dielectric spectroscopy investigations of liquid vein networks within ice and ice-regolith mixtures. In: 50th lunar and planetary science conference, abs. 2537.
Stuurman, C.M., Osinski, G.R., Holt, J.W., Levy, J.S., Brothers, T.C., Kerrigan, M., Campbell, B.A., 2016. SHARAD detection and characterization of subsurface water ice deposits in utopia Planitia. Mars. Geophys. Res. Let. 43 (18), 9484–9491. https://doi.org/10.1002/2016GL070138.
Sutter, B., McAdam, A.C., Rampe, E.B., Thompson, L.M., Ming, D.W., Mahaffy, P.R., Navarro-Gonzalez, R., Stern, J.C., Eigenbrode, J.L., Archer, P.D., 2017. Evolved gas analyses of the Murray formation in Gale crater, Mars: results of the curiosity rover's sample analysis at Mars (SAM) instrument. In: 48th lunar and planetary science conference, Abs. 3009.
Tamppari, L.K., Anderson, R.M., Archer, P.D., Douglas, S., Kounaves, S.P., McKay, C.P., Ming, D.W., Moore, Q., Quinn, J.E., Smith, P.H., Stroble, S., Zent, A.P., 2012. Effects of extreme cold and aridity on soils and habitability: McMurdo dry valleys as an analogue for the Mars Phoenix landing site. Antarct. Sci. 24 (3), 211–228. https://doi.org/10.1017/S0954102011000800.
Toner, J.D., Catling, D.C., 2018. Chlorate brines on Mars: implications for the occurrence of liquid water and deliquescence. Earth Planet. Sci. Lett. 497, 161–168. https://doi.org/10.1016/j.epsl.2018.06.011.
Toner, J.D., Catling, D.C., Light, B., 2014a. The formation of supercooled brines, viscous liquids, and low-temperature perchlorate glasses in aqueous solutions relevant to Mars. Icarus 233, 36–47. https://doi.org/10.1016/j.icarus.2014.01.018.
Toner, J.D., Catling, D.C., Light, B., 2014b. Soluble salts at the Phoenix Lander site, Mars: a reanalysis of the wet chemistry laboratory data. Geochim. Cosmochim. Acta 136, 142–168. https://doi.org/10.1016/j.gca.2014.03.030.
Toner, J.D., Catling, D.C., Light, B., 2015. A revised Pitzer model for low-temperature soluble salt assemblages at the Phoenix site, Mars. Geochim. Cosmochim. Acta 166, 327–343, 10.106/j.gca.2015.06.011.
Tosca, N.J., Knoll, A.H., McLennan, S.M., 2008. Water activity and the challenge for life on early Mars. Science 320, 1204–1207. https://doi.org/10.1126/science.1155432.
Weast, R.C. (Ed.), 1987. *CRC Handbook of Chemistry and Physics* 68th Edition, D219-D269. CRC Press, Boca Raton.
Wettlaufer, J.S., Worster, M.G., 2006. Premelting dynamics. Annu. Rev. Fluid Mech. 38, 427–452. https://doi.org/10.1146/annurev.fluid.37.061903.175758.
Zent, A.P., 2008. A historical search for habitable ice at the Phoenix landing site. Icarus 196, 385–408. https://doi.org/10.1016/j.icarus.2007.12.028.
Zent, A.P., Hect, M.H., Cobos, D.R., Wood, S.E., Hudson, T.L., Milkovich, S.M., DeFlores, L.P., Mellon, M.T., 2010. Initial results from the thermal and electrical conductivity probe (TECP) on Phoenix. J. Geophys. Res, Planets 115. https://doi.org/10.1029/2009JE003420.